

8-2017

Experiment-Based Quantitative Modeling for the Antibacterial Activity of Silver Nanoparticles

Mohammad Aminul Haque
University of Arkansas, Fayetteville

Follow this and additional works at: <http://scholarworks.uark.edu/etd>

 Part of the [Biophysics Commons](#), and the [Nanoscience and Nanotechnology Commons](#)

Recommended Citation

Haque, Mohammad Aminul, "Experiment-Based Quantitative Modeling for the Antibacterial Activity of Silver Nanoparticles" (2017). *Theses and Dissertations*. 2445.
<http://scholarworks.uark.edu/etd/2445>

This Thesis is brought to you for free and open access by ScholarWorks@UARK. It has been accepted for inclusion in Theses and Dissertations by an authorized administrator of ScholarWorks@UARK. For more information, please contact scholar@uark.edu, ccmiddle@uark.edu.

Experiment-Based Quantitative Modeling for the Antibacterial Activity of Silver Nanoparticles

A thesis submitted in partial fulfillment
of the requirements for the degree of
Master of Science in Electrical Engineering

by

Mohammad Aminul Haque
University of Dhaka
Bachelor of Science in Applied Physics, Electronics and Communication Engineering, 2014

August 2017
University of Arkansas

This thesis is approved for recommendation to the Graduate Council

Dr. Yong Wang
Thesis director

Professor Morgan Ware
Committee member

Dr. Zhong Chen
Committee member

Abstract

Silver (Ag) has been well known for its antimicrobial activity for a long time. Recent research showed the potential of Ag nanoparticles as emerging antimicrobial agents. However, little quantitative analysis has been performed so far to decipher the mechanism of interaction between nanoparticles and bacteria. Here, a detailed analysis based on kinetic growth assay and colony forming unit assay has been carried out to study the antimicrobial effect of Ag nanoparticles against *Escherichia coli* (*E. coli*) bacteria. It was observed that the presence of Ag nanoparticles increased the lag time of bacterial growth while not affecting the maximum growth rate significantly. Besides, they can inhibit bacterial growth in the exponential phase by killing some *E. coli* bacteria cells. A quantitative model was developed to describe the observed antimicrobial behaviors of Ag nanoparticles. The model can successfully predict the experimental measurements. In addition, a mathematical approach to extract the model parameters using experimental data has also been described. It is expected that the model along with the parameters will help to understand the antimicrobial activity of Ag nanoparticles.

Acknowledgments

I would like to express my gratitude to my advisor Dr. Yong Wang for his continuous support and mentorship throughout my MSEE study. I am also thankful to other members in my thesis committee for their suggestions. I am grateful to my parents for their support and guidance. Special thanks to my lab coworkers for their help and support during the experiments. I would also like to thank my friends for their suggestions and encouragement towards completing this thesis work.

Table of Contents

CHAPTER ONE	1
Introduction	1
1.1 History of using antimicrobial agents	1
1.2 Silver nanoparticles	5
1.3 Applications of nanoparticles against bacteria	6
1.4 Mechanism of silver-bacteria interaction	9
1.5 Motivation of the work	11
CHAPTER TWO	12
Experiment.....	12
2.1 Synthesis of silver nanoparticles (AgNPs)	12
2.2 Characterization of silver nanoparticles (AgNPs).....	13
2.3 Growth of bacteria.....	16
2.4 Kinetic Growth Curve Experiments	17
2.5 CFU Assay and Time Kill Measurements	18
CHAPTER THREE.....	20
Experimental observations and data analysis	20
3.1 Kinetic Growth Curve assay:	20
3.2 Colony Forming Unit (CFU) assay	22
3.2 Time-kill curves:	33
CHAPTER FOUR.....	40

Quantitative Model and Verification	40
4.1 Proposed Quantitative model:	40
4.2 Application in experimental condition for Verification	43
4.3 Parameter extraction and Application	47
CHAPTER FIVE	59
Discussion and Conclusion.....	59
References	61
Appendix	67

List of Published Papers

1. M. Haque, R. Imamura, G. A. Brown, T. Marcelle, J. Chen, and Y. Wang, “An Experiment-Based Quantitative Model Describing Antimicrobial Activity of Silver Nanoparticles on *Escherichia coli*,” *Sci. Rep.*, 2017, under review.

CHAPTER ONE

Introduction

1.1 History of using antimicrobial agents

Different plants were used to heal wounds thousands of years ago [1]. Allantoin is found in Comfrey (*Symphytum officinale*) which is antibacterial as well as a healing agent [1]. Leaves of St John's wort (*Hypericum perforatum*) are also supposed to have some healing effect in perforating wound [1]. Grasses have always been used as bandages for soothing [1]. Honey, animal fats and butter were later used in wound treatment [1]. Antagonistic behavior of some microorganisms against bacteria was first observed by William Roberts (1874) and John Tyndall (1876) [2]. Roberts reported inhibition of bacteria on *Penicillium glaucum* covered media and Tyndall was able to explain the hostility between bacteria and moulds (multicellular filament fungus) [2]. In 1897, Ernest Duchesne, while working towards his PhD, observed the antimicrobial activity of *Penicillium glaucum* [3]. This is the first known published research on the antimicrobial activity of moulds [3]. In 1928, Sir Alexander Fleming proposed the existence of penicillin in *Penicillium chrysogenum* secretion preventing the growth of bacteria [4]. The improvement in this field encouraged the scientists to pursue further research for more antibiotics [5]. In 1939, Rene Dubos was able to synthesize the first naturally derived antibiotic, tyrothricin [6]. It contained gramicidin and tyrocidine [6]. Tyrocidine attacked both gram-positive and gram-negative bacteria whereas gramicidin was able to inhibit gram-positive bacteria [6]. In fact, gramicidin was used to treat wounds and ulcers during World War II [6]. However, it was not suitable against systemic infections due to toxicity [6].

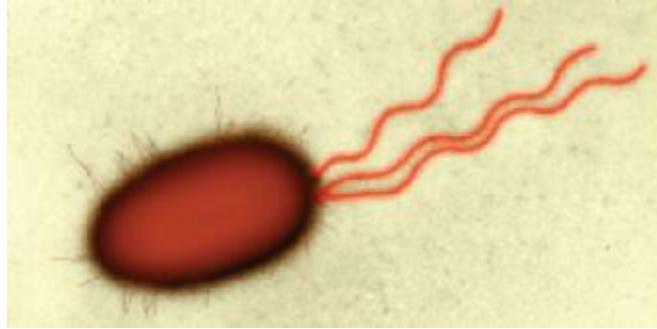


Fig. 1.1: A magnified electron microscopic image of *E. coli* [7]

E. coli, discovered by Theodor Escherich in 1885, is a rod-shaped gram-negative bacterium frequently found in lower intestine of warm-blooded lives [8]. Although most of them are found inside the body, they are capable of surviving outside the body [9]. They are 2 μm long, 0.5-2 μm in diameter while the cell volume is 0.6-0.7 μm^3 [9]. Most frequently used temperature for *E. coli* growth is 37 $^{\circ}\text{C}$ [9]. *E. coli* can transfer DNA from generation to generation through conjugation, transduction or transformation [9]. Bacterial strains (sub-type of bacteria having exclusive properties to differentiate from other strains) are host specific [9]. By knowing which strain is present in human body, it can be determined where the contamination arises from (for instance, from another human or animal) [9]. Although use of temperature beyond 37 $^{\circ}\text{C}$ is not recommended for *E. coli* growth, protocol has been developed to grow *E. coli* (DH5alpha) up to 49 $^{\circ}\text{C}$ [10]. It means that *E. coli* (DH5alpha) can go through mutation that enables them to grow at temperature beyond 37 $^{\circ}\text{C}$ [10]. *E. coli* can grow in any medium (for instance, LB) containing ammonium phosphate, sodium chloride, magnesium sulfate, potassium phosphate, glucose and water. Both aerobic and anaerobic respiration can drive the growth of *E. coli* [11]. *E. coli* is termed as facultative anaerobic. It uses oxygen for growth wherever it is present. However, it can

still grow through anaerobic respiration if oxygen is present. Therefore, its growth is accelerated if water increases in the environment [12].

Many of the *E. coli* bacteria are nonpathogenic and can be good source of vitamin K₂ thereby benefitting the host [13]. However, some can cause food contamination and food poisoning [14]. Harmful strains can cause gastroenteritis, urinary tract infections, neonatal meningitis etc [15]–[17]. Gastroenteritis is a complex biological response of stomach and small intestine to pathogens or damaged cells [18]. Vomiting, diarrhea, abdominal pain and fever are some of the common syndromes [18]. When part of the urinary tract (kidneys, bladders, ureters and urethra) is affected by bacterial infection, it is termed as urinary tract infection [19]. Bladder infection (cystitis) occurs when lower urinary tract is affected whereas infection in the upper urinary tract is called kidney infection (pyelonephritis) [20]. Pain with urination, frequent urination and fever are some symptoms of urinary tract infection [19], [20]. Neonatal meningitis is a complex response of the meninges (membranes protecting brain and spinal cords) and a serious medical problem in infants [21]. The possible symptoms are fever, poor appetite, vomiting, diarrhoea, neck rigidity, jaundice etc. [15]–[17], [22]. Properly cooking food, use of gloves, clean drinking water, pasteurization etc are some of the ways to prevent contamination [9].

E. coli has been widely used in research for the following reasons:

- *E. coli* has small genome size with respect to eukaryotes. They have about 4400 genes whereas humans have almost 30000 genes [23], [24].

- *E. coli* can grow at the rate of one generation per twenty minutes in regular growth conditions. This allows for preparation of high-density cultures overnight rather than waiting for weeks or months [23].
- *E. coli* are generally innocuous when handled with hygiene [23].
- *E. coli* can be easily transformed with plasmids and other vectors. Transformations with other bacteria are often less successful [23].

Herodot first mentioned the use of silver container for water transportation [25]. The Greeks, the Romans and the Egyptians used silver for water and food conservation [26]. Being a noble metal, silver is generally not affected by acid or water. But it can release some metal ions which account for antimicrobial activity on the metal surface [25]. Metallic silver (Ag) and silver ions (Ag⁺) have been used for its resistive activity against microorganisms such as bacteria [27]. Nowadays, various biomedical applications such as dental treatment and catheters take advantage of bacterial suppression by Ag⁺ [27]. Ag has also been used in refrigerators, dishwashers and other electrical appliances [27]. In addition to Ag⁺ ions, Ag nanoparticles have also shown significant bacterial suppression [27].

Change in chromosomes and genetic materials through plasmids and transposons (another DNA sequence, capable of altering cell's genetic identity and mutations) from time to time have made bacteria resistant to antimicrobials agents [28]. Bacteria causing respiratory and urinary infections and diarrhea became resistant to all older antibiotics by 1992 [28]. This led to decrease in approved number of antibiotics in US and subsequent increase in threat to public health [29]. It requires the research for potential new antimicrobial agents and new bacteria treatment approaches [29]. These include modifying existing antibiotics as well as searching for new

naturally obtained antimicrobials [29]. Nanoparticles provide specific advantage in terms of fighting bacteria due to their unique physical attributes such as smaller dimension, higher surface to volume ratio etc. [29]. Nanoparticle dimension is in the same proportion of bacterial sizes and systems thereby providing more interactions with nanoparticles [29]. The high surface to volume ratio of nanoparticles increases the number of effective ligands (and therefore, more valence bonds) on the surface [29]. This incorporates increased number of bacterial interactions [29]. Based on these properties, nanoparticles have been incorporated with antibiotics using both covalent and noncovalent bonds for increased activity against bacteria [29]. Several previous experiments showed the antibacterial activities of Nanoparticle also [30]–[32].

1.2 Silver nanoparticles

The release of silver from nanoparticle depends on the size and surface functionalization of the nanoparticles, temperature and composition of ambient medium [33], [34]. Silver nanoparticles (AgNPs) are known for 120 years [35]. Ag nanomaterials can be synthesized in both ‘bottom-up’ and ‘top-down’ approaches [36]. The top down method consists of bulk metal grinding followed by stabilization of metal particles by using protecting agents [36]. In the bottom-up approach, Ag nanoparticles can be obtained from reduction of metals, electrochemical methods or sonodecomposition [36]. Commonly, Ag nanoparticles are synthesized by reducing soluble silver salts with agents like ethylene glycol, glucose, citrate etc. [25]. Different types of Ag nanoparticles, such as sphere, bipyramid [37], discs [38], rods [39], cubes can be found in literature based on the conditions of reaction [25].

AgNPs show distinctive optical properties [40]. When exposed to electromagnetic radiation, their conduction electrons behave as surface plasmon polariton resonances [40]. This property

depends on specific factors like: acceleration of conduction electrons by incident electric field, restoring forces due to polarization and electron confinement within dimension smaller than the wavelength of light [40].

Ag has been used for antimicrobial application for hundreds of years [25], [26]. Despite the antimicrobial activity of Ag, they can be harmful to humans and nature also [36]. The toxic nature of AgNPs has been a major concern in its application [41], [42]. It has been reported that AgNPs need to release Ag^+ ions before behaving as toxic material and they cannot produce toxicity in only nanoparticle form [41]. However, when they produce such toxicity, they can cause damage to human cells [42]. It can damage mitochondria and increase reactive oxygen production based on amount of dose [42]. It also accounts for dose dependent DNA damage which is more prominent in cancer cells [42]. Besides, AgNPs stored in laboratory gradually release Ag^+ ions over time thereby showing more toxicity to human cells than fresh AgNPs [43].

A large amount of Ag that is dumped as industrial waste accounts for the increased toxicity in the environment [36]. The detrimental effects on humans and other living species include the discoloration of skin (argyria) and (argyrosis) [36]. Moreover, soluble silver can cause liver and kidney damage, respiratory and intestinal tract irritations etc. [36], [44].

1.3 Applications of nanoparticles against bacteria

Comprehensive research on the antimicrobial activity of Ag nanoparticles started developing around 2004 [30], [45]. Both antimicrobial efficacy and antimicrobial mechanism of AgNPs have been studied in recent years [30]–[32], [46]–[49].

Antibacterial mechanism of nanoparticles have been tested against Bacillus Calmette-Guerin (BCG, used as a substitute of TB for developing anti-TB drug) [31]. BCG can be developed from *Mycobacterium bovis* [31]. *Mycobacterium bovis* is the cause of bovine tuberculosis [31]. Single drug therapy often fails to remove infection as well as giving rise to antibacterial resistance [31]. This leads to the use of multi-drug therapy method [31]. However, phenomena like drug induced disease and presence of multidrug resistant bacteria have obliged researchers to look for new approaches [31]. Silver attacks multiple components in a bacterial cell, so cells cannot be readily resistive to silver [31]. Both gold and silver NPs have been tried before to some extent to observe their antibacterial activity using similar size and shapes [31]. Their growth was observed by the method of Colony Forming Units (CFU) [31]. In CFU assay, agar (a semisolid base) is first mixed with a nutrient medium and then poured onto a petri dish [50]. The solution solidifies on the petri dish as it cools down [50]. A dilute bacterial culture is then spread over the solidified nutrient medium where each cell grows into a separate colony over time [50]. Since all the cells in the colony grow from a single cell, they have homogeneous DNAs [50]. Each colony is formed over time and they can be counted either manually or by using software to get an estimation [51]. Both transmission electron microscopy (TEM) and field emission scanning electron microscopy (FE-SEM) were used to analyze the dynamics of bacteria-NP interaction [31]. It shows the potential of using NP against multi drug resistant bacteria [31].

AgNPs have been extracted from *Trianthema decandra* (saponin) and their antimicrobial activity was observed using Kirby–Bauer method [32]. The antimicrobial activity was observed against 8 different bacteria, where it was found that antimicrobial activity was more conspicuous against gram-negative bacteria than gram positive bacteria [32]. The size of AgNPs is 250 times smaller

than a bacterium (37.7–79.9 nm) enabling it to easily stick to the cell walls resulting the death of the cell [32].

NP toxicity on bacteria depends on both bacteria type and size, shape, surface charge and chemical composition[52]. The bacteriostatic and bactericidal effects depends for by the size and dose of the AgNPs [46]. Both Minimum Inhibitory Concentration (MIC) and Minimum Bactericidal Concentration (MBC) against a specific bacterial strain account for the size and dose of Nanoparticle to be used [46]. The efficacy of nanoparticles increases with decrease in dimension as 10 nm and lower dimensional nanoparticles have been more effective than the higher ones [46]. Different shapes of AgNPs were tested against *E. coli* to determine the significance of shape on its antimicrobial activity [47]. Nanoscale size and presence of {111} plane were proposed to govern the biocidal efficiency of AgNPs [47]. Therefore, it was reported that AgNPs exhibit shape-dependence antimicrobial activity against gram-negative *E. coli* [47]. *Escherichia coli* (*E. coli*) and *Staphylococcus aureus* (*S. aureus*) were found to be the most and least affected by Nanoparticles respectively [46].

Apart from *E. coli* and *S. aureus*, *Enterococcus faecalis* (*E. faecalis*) was also tested against AgNPs to determine its MIC and MBC against *E. faecalis* [48]. 5 µg/mL was detected as MIC and MBC of AgNPs against *E. faecalis* thereby validating the potential bactericidal effects of AgNPs [48]. Therefore, it was proposed in intra canal medicaments as irrigants [48].

To observe the antimicrobial mechanism of AgNPs on microorganisms, yeast, *E. coli* and *S. aureus* were treated with AgNPs [49]. Yeast and *E. coli* were found to be inhibited by low concentrations of AgNPs [49]. However, growth-inhibitory effect on *S. aureus* was mild [49].

Electron beam resonance spectroscopy was used to analyze the free-radical generation by AgNPs

[49]. The results suggested the potential use of AgNPs against microorganisms [49]. To explore further mechanism, surface properties and the parameters that affect the surface states of AgNPs were studied [30]. These properties are believed to influence the release of Ag^+ ions thereby regulating the potential antimicrobial mechanism [30].

1.4 Mechanism of silver-bacteria interaction

Gram-negative bacteria was exposed to different concentrations of AgNPs and their effect was observed using both scanning electron microscopy (SEM) and transmission electron microscopy (TEM) [45]. It was found that the nanoparticles penetrated through the cell walls to the membranes to cause death of bacteria cells [45]. Combining focused ion beam (FIB), scanning electron microscopy and energy dispersive X-ray spectroscopy, Ag nanoparticles can be traced inside a cell [25]. Inside the cell, presence of silver causes the condensation of DNA [53]. DNA replication (and subsequent cell growth) takes place when a relaxed state prevails in DNA [53]. Condensation of DNA restrains DNA molecules from replication, leading to ultimate death of the cell [53].

Therefore, death of a cell through interaction with AgNP appears to be associated with the structure of DNA. DNA (Deoxyribonucleic Acid) contains all the genetic information and instructions regarding growth and functioning of all living organisms [7]. Two biopolymer strands spiral around each other to form the double helix structure of DNA [54]. Nucleotides accumulate together to form these DNA strands [54]. Therefore, they are called polynucleotides [54]. Each nucleotide consists of a sugar group (deoxyribose), a phosphate group and one of the four nitrogen-containing nucleobases (Adenine, Thymine, Guanine and Cytosine) [7]. Each DNA string coils around a cylindrical protein (Histones) forming a Chromatin [7]. The

chromatin further convolutes to develop a condensed structure called Chromosome [7]. One of the many differences between bacteria and other cells is the presence of Plasmid[55]. Plasmids are also small DNA structures (double-stranded) found in bacteria cells [55]. However, they are physically isolated from chromosomal DNA and capable of replicating themselves independently [56]. They carry only additional genes (not the essential genetic information like chromosomal DNA) to help them survive in particular conditions [56].

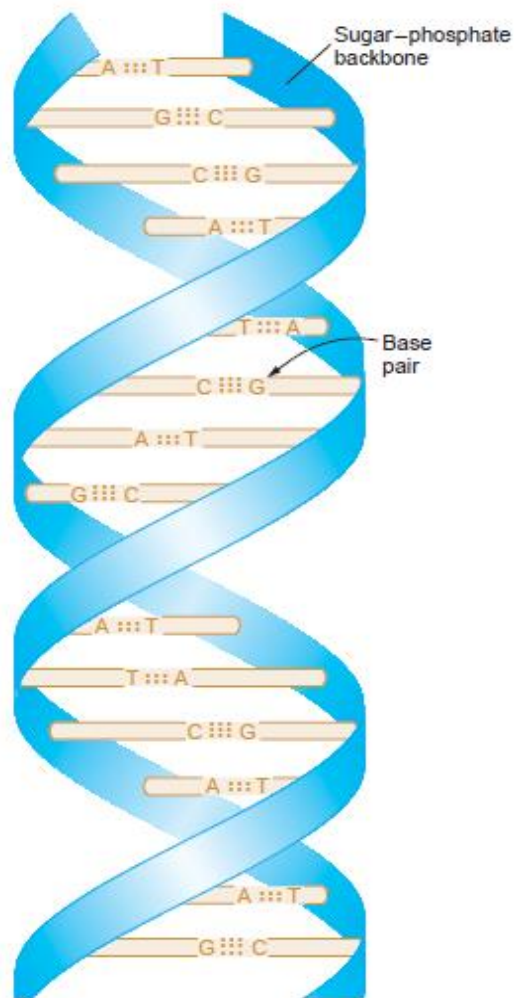


Figure 1.2: A simplified model of a helical DNA. Sticks and ribbons represent The base pairs and sugar phosphate backbones respectively [7]

Inclusion of amino-substituted pyrimidines with gold nanoparticles were effective against multi drug resistant bacteria [57]. These pyrimidines do not have bactericidal effect on their own [57]. However, pyrimidine capped nanoparticles damage bacterial cell membrane using magnesium or calcium [57]. This proves that nanoparticles are the ones that are responsible for the bacteria cell membrane damage [57].

1.5 Motivation of the work

Although Ag has been used extensively to treat wounds for a long time, antimicrobial mechanism of Ag nanoparticles has not been persistently described [32]. Based on the literature reviewed so far, research on antimicrobial mechanism of AgNPs has been focused on two directions: exploring efficiency of AgNPs as potential antimicrobials and investigating experiment-based antimicrobial mechanism of AgNPs [30]–[32], [45]–[48], [53], [58]. Despite these advancements, little quantitative analysis has been performed so far regarding the antibacterial mechanism of Nanoparticles. A quantitative approach would help to characterize the antimicrobial activity of nanoparticles. Moreover, a quantitative model would help to understand and predict the antimicrobial behavior of AgNPs in specific growth medium. In this work, kinetic growth assays and CFU assays were performed using AgNPs against *E. coli* bacteria. Based on the experimental observations, a quantitative approach has been undertaken for better understanding of experimental findings. It was found that the presence of AgNPs mainly affected the lag time instead of the growth rate of the bacteria. A quantitative model has been developed to explain these experimental observations.

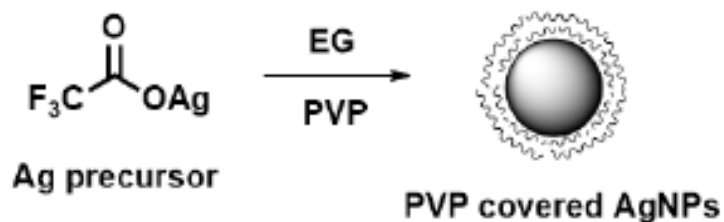
CHAPTER TWO

Experiment

2.1 Synthesis of silver nanoparticles (AgNPs)

In this study, AgNPs were synthesized using polyol method with poly (vinylpyrrolidone) as the capping agent (Fig. 2.1). Polyol method is the synthesis of metal-containing compounds in poly (ethylene glycol)s, which act as both the solvent and reducing agent [59]. It was first introduced to produce fine metal powders such as Copper (Cu), Gold (Au), Palladium (Pd), Ag, Cobalt (Co), Nickel (Ni), Iron (Fe) and their alloys [59]. This method is considered as an apparently easy method among all the physical, chemical or electrochemical processes [60].

A 250 mL round-bottom flask with a stirring bar was set up in a 150 °C oil bath, followed by the addition of 50 mL ethylene glycol (EG, J.T. Baker). As the temperature reaches equilibrium (after 30~45 minutes), EG solutions of 0.6 mL of 3 mM NaHS (Alfa Aesar), 5 mL of 3 mM HCl (Alfa Aesar), 12.5 mL of 0.25 g poly(vinylpyrrolidone) (PVP, M.W.=55,000, Sigma-Aldrich), and 4 mL of 282 mM silver trifluoroacetate (AgTFA, Alfa Aesar) were added successively one after another. It was damped in an ice bath after the peak of localized surface plasmon resonance (LSPR) reached ~430 nm. When it was cooled, acetone was added to the reaction with a ratio of 5:1 and centrifuged at 6000 rcf (Relative Centrifugal Force) to collect the product. The resulting pellet was purified twice by re-suspension in water and centrifugation at 20000 rcf for 10 min. The final pellet was re-suspended in 10 mL of water for later use.



EG: ethylene glycol (reducing agent)
 PVP: poly(vinylpyrrolidone) (stabilizer)

Fig. 2.1: Schematic representation of the reaction to produce AgNP

2.2 Characterization of silver nanoparticles (AgNPs)

The synthesized nanoparticles have been characterized by various techniques as shown below.

- Transmission Electron Microscopy (TEM) was used to image the synthesized AgNPs using a TEM microscope (JEOL JEM-1011) with an accelerating voltage of 100 kV. A typical TEM image is shown in Fig. 2.2, where irregular shapes of the AgNPs were observed: spheres, short rods, triangles and tetrahedrons. The sizes of the AgNPs in the TEM images were analyzed and we determined that the average diameter of the NPs was 39.5 ± 10.7 nm. The distribution of the size of AgNPs was shown in Fig. 2.3, indicating two peaks at ~ 30 nm and ~ 50 nm.

- The size of the AgNPs were measured independently with another technique, dynamic light scattering (DLS), which has been commonly used for determining the hydrodynamic diameter (i.e., size) of small particles, polymers, and biological macromolecules in aqueous solutions [61]. The hydrodynamic diameter of our AgNPs was measured with Brookhaven ZetaPALS), giving a size distribution as shown in Fig. 2.3. The average size was found to be ~ 69 nm with the polydispersity index (PDI) of 0.327. Polydispersity means the distribution of

molecular mass or shape in the sample and high value of PDI proves the existence of polydispersity in our sample. The polydispersity index is dimensionless and a value greater than 0.7 suggests a very broadly distributed sample thereby being not suitable for DLS [62]. Since DLS assumes all the particles as spherical, it may not accurately estimate the size of the irregular nanoparticles.

- The silver concentration of our AgNPs stock solution was measured by atomic absorption spectroscopy [63]. A flame atomic absorption (AA) spectrometer (GBC 932) was used, and we determined that the concentration was 2500 ppm ($\mu\text{g}/\text{mL}$). .

- The composition of our AgNPs was determined by X-ray powder diffraction (XRD), which is a convenient tool to determine the spacing between lattice planes (h, k, l - miller indices) thereby confirming the existence of a specific material [64]. For a face centred cubic structure, all of h, k and l have to be either odd or even [64]. We measured peaks at 38.04, 44.22, 64.34, 77.24, and 81.38 degree (Fig. 2.4), which correspond to {111}, {200}, {220}, {311}, and {222} crystallographic planes. The X-ray diffraction result confirmed the existence of metallic face centred cubic Ag in the sample (200, 220, 222 - all even and 111, 311 – all odd).

- To characterize the charges on our AgNPs, we also measured the zeta potential of the AgNPs. When a particle is dispersed in a medium, a conventional slipping plane separates between the mobile fluid and the fluid attached to the surface. The electric potential between the dispersion medium and this plane is called zeta potential [65]. The zeta potential of our AgNPs was determined as $-8.50 \text{ mV} \pm 2.04 \text{ mV}$, which shows that PVP-capped AgNPs are somewhat negatively charged as found in the literature also [66].

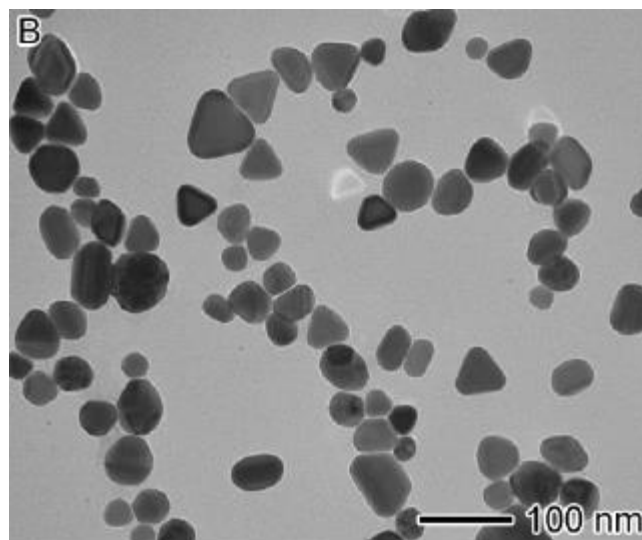


Fig. 2.2: Transmission Electron Microscope (TEM) photograph of AgNPs

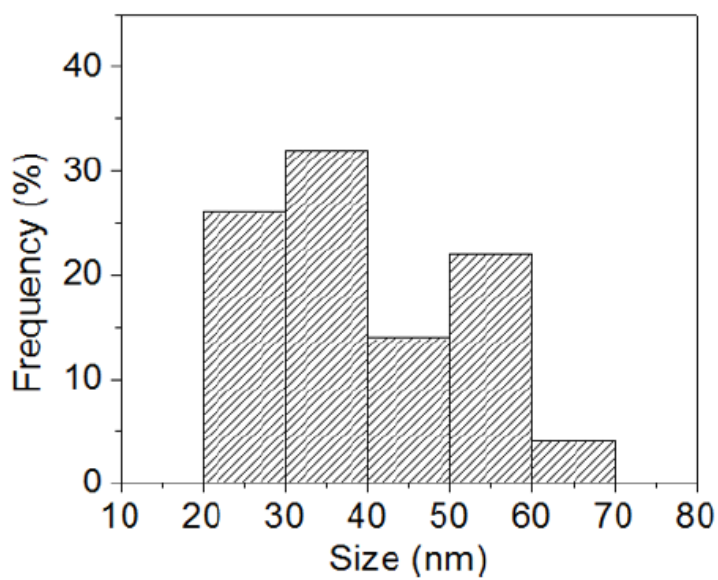


Fig. 2.3: Size distribution of AgNPs from the TEM image in Fig. 2.2

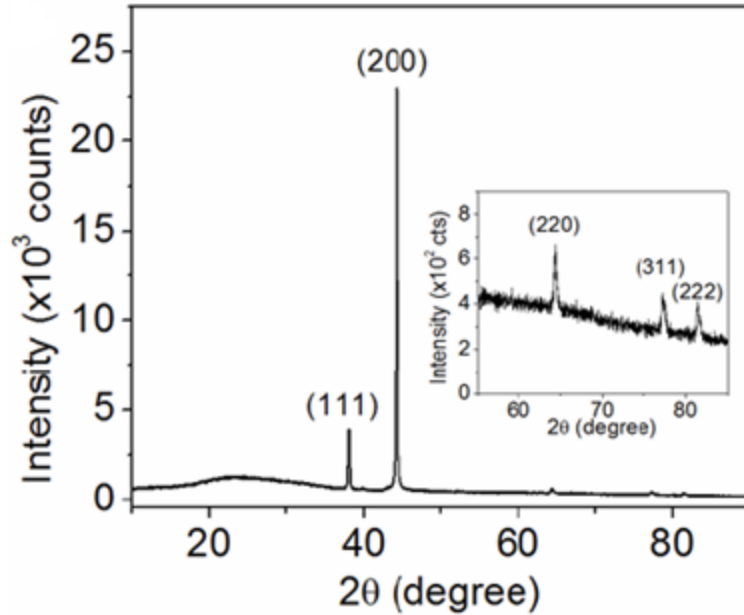


Fig. 2.4: X-ray powder diffraction pattern of AgNPs

2.3 Growth of bacteria

The following bacteria, antibiotic and medium were used for the growth of bacteria in this study.

- DH5 α is an *E. coli* strain that is most frequently used in cloning application. It contains multiple mutations enabling high-efficiency transformations [64].
- Ampicillin is an antibiotic used against infections from both gram-positive (*Streptococcus pneumoniae*, *Staphylococcus aureus* etc.) and gram-negative (*Neisseria meningitidis*, *Haemophilus influenzae* etc.) bacteria. It is regarded as one of the most effective and safe medicines for a health system [67].
- Plasmid pOEGFP2 (a gift from Dr. David McMillen at the University of Toronto) carries ampicillin resistance and Enhanced Green Fluorescent Protein (EGFP). Green Fluorescent Protein (GFP) is a protein first collected from the jellyfish *Aequorea victoria* [68]. Its emission

peak (509 nm) is in the lower green part of the visible spectrum [68]. Therefore, when it is exposed to light from blue to ultraviolet range, it shows bright green fluorescence [68].

- Lysogeny broth (or Luria broth, LB) is an industry standard nutritionally rich medium widely accepted and used for the growth of *E. coli* [69].

Escherichia Coli bacteria DH5 α (Thermo Fisher Scientific) was transformed by plasmid pOEGFP2 carrying ampicillin resistance and Enhanced Green Fluorescent Protein (EGFP). This bacteria was grown overnight in LB medium (EMD Millipore) containing 100 $\mu\text{g/mL}$ (standard working concentration) ampicillin (G-Biosciences) in an orbital shaking incubator (Thermo Scientific) at 37 °C and 250 rotation per minute (rpm). The green fluorescence of pOEGFP2 was convenient for verification. Next day, concentration of the overnight culture (OD_{600}) was first determined using a NanoPhotometer C40 (Implen Inc.). It was then diluted into LB medium to achieve the desired concentration. This time, instead of ampicillin, AgNPs or Ag⁺ ions (in form of AgNO₃) was added to the LB medium. These new cultures were incubated in the shaking incubator again at 37 °C and 250 rpm. The new cultures were used in the kinetic growth curve experiments and/or colony forming unit experiments, as described below.

2.4 Kinetic Growth Curve Experiments

In a typical kinetic growth curve experiment, the growth of the second-day cultures was monitored by measuring the concentration (OD_{600}) using the NanoPhotometer C40 every 45 minutes for 12 hours and then at 24 hour, 30 hour and 36 hour time periods. For the kinetic growth curve experiments with fixed initial concentration of bacteria, the overnight culture was diluted to achieve OD_{600} value of 0.05. The concentrations used for AgNPs were 0, 1, 5, 10, 20,

30, 40 $\mu\text{g}/\text{mL}$ and for AgNO_3 , the concentrations were 0, 1, 2, 5, 7, 10 $\mu\text{g}/\text{mL}$. For the experiments with varying initial concentrations of bacteria, the fixed initial concentration was 20 $\mu\text{g}/\text{mL}$ for AgNPs and 5 $\mu\text{g}/\text{mL}$ for AgNO_3 . The varying initial OD_{600} concentrations of *E. coli* bacteria were 0.001, 0.005, 0.01, 0.05, 0.1, and 0.2.

For the experiments for halted growth of *E. coli* bacteria in the exponential phase, the procedures were similar as the experiments for lag phase (i.e., $\text{OD}_{600} = 0.05$). The overnight culture was diluted in LB medium to achieve the concentration of $\text{OD}_{600} = 0.05$ and allowed to grow in the shaking incubator at 250 rpm and 37 °C until it reached the OD_{600} value of ~ 0.5 . Then AgNPs were added to the sample so that the final concentrations of AgNPs become 0, 20, 40, 80 $\mu\text{g}/\text{mL}$. For Ag^+ ions, the final concentrations were 0, 10, 20, 40, 60 $\mu\text{g}/\text{mL}$. OD_{600} values of these samples were measured every 45 minutes for ~ 15 hours using NanoPhotometer C40.

2.5 CFU Assay and Time Kill Measurements

For CFU assay and time kill measurements, *E. coli* bacteria DH5 α containing plasmid pOEGFP2 were grown overnight in LB medium with ampicillin (working concentration=100 $\mu\text{g}/\text{mL}$) in a shaking incubator at 37 °C and 250 rpm. On the second day, overnight culture was diluted in fresh LB medium to achieve OD_{600} concentration of 0.05. It was allowed to grow in the shaking incubator at 250 rpm and 37 °C until it reaches 0.3-0.5. Then it was diluted again to 0.005 and AgNPs or Ag^+ ions were added to it to the desired concentration. The samples were taken back to the incubator at 37 °C and 250 rpm. A small volume was taken at different time intervals (0, 1, 2, 3, 4 ... hours) and diluted in LB medium 100-10000 times. 100 μL of each dilution was plated on LB agar plates and incubated at 37 °C. Ampicillin (working concentration = 100 $\mu\text{g}/\text{mL}$) was

added while preparing the LB agar plates to avoid contamination. The number of colonies on the LB agar plates was counted manually the next day.

CHAPTER THREE

Experimental observations and data analysis

3.1 Kinetic Growth Curve assay:

Previous works included the synthesis of AgNPs from *Lycopersicon esculentum* (Red tomato). To observe their antimicrobial activity, *E. coli* was inoculated on LB agar plates at presence of different AgNP concentrations. The MIC (Minimum Inhibitory Concentration) was determined as 50 $\mu\text{g/mL}$ [70]. These previous results were first verified through kinetic growth curve assay and CFU assays. For the kinetic growth curve assay, bacterial cell density was observed through measuring the OD_{600} values of the solutions.

In the kinetic growth curve consisting of different concentrations of AgNPs and an initial bacteria $\text{OD}_{600} = 0.05$, it was observed that 40 $\mu\text{g/mL}$ AgNPs was able to suppress the growth of bacteria for 12 hours (Fig. 3.1). For lower concentrations (20 and 30 $\mu\text{g/mL}$), the growth of bacteria was temporarily suppressed; they started growing later on (Fig. 3.2). However, for concentrations below 10 $\mu\text{g/mL}$, no significant suppression was observed.

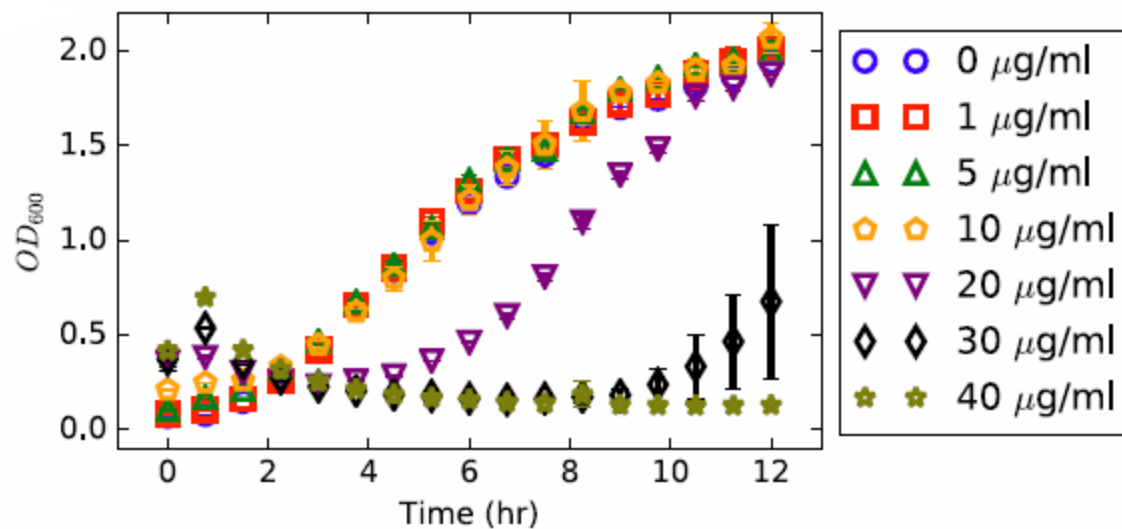


Fig. 3.1: Suppression of the growth of bacteria by different concentrations of AgNPs (up to 12 hours)

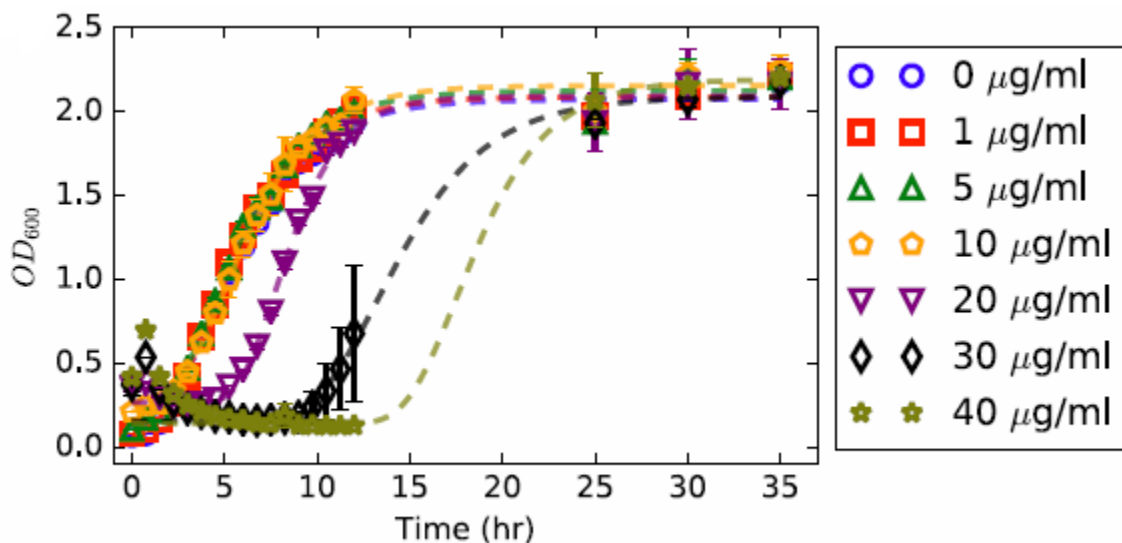


Fig. 3.2: Suppression of the growth of bacteria by different concentrations of AgNPs, fitted with Gompertz model (up to 36 hours)

3.2 Colony Forming Unit (CFU) assay

For further verification of suppression, CFU assays were performed with AgNPs (0, 10, 20, 40 $\mu\text{g}/\text{mL}$, Fig. 3.4) and Ag^+ ions (0, 2, 5, 10 $\mu\text{g}/\text{mL}$, in AgNO_3 form in Fig. 3.5). In CFU assay, the growth of *E. coli* was also suppressed in presence of AgNPs thereby producing similar results (Fig. 3.4). These results were consistent with previous reports found on literature [31], [45], [71]. The number of colonies should vary linearly with the estimated concentration of the culture since they are diluted from the same bacteria culture. The CFU assays concur with this concept as we can see from Fig. 3.3 where number of colonies are plotted against estimated concentration of the culture.

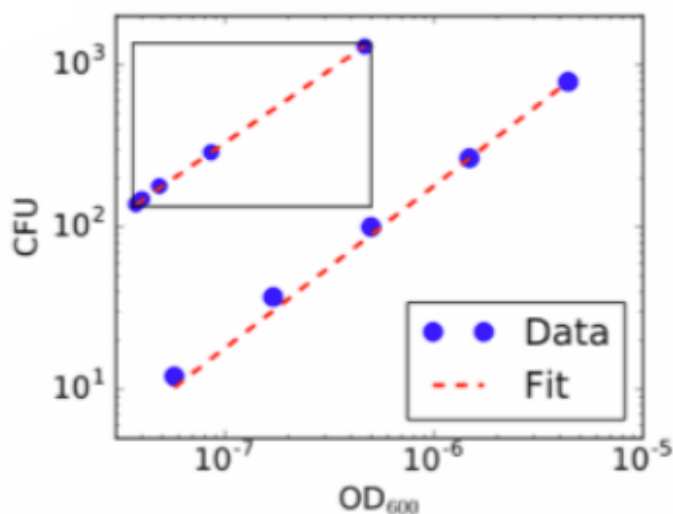


Fig. 3.3: Relation between number of colonies and concentration of diluted culture in the log scale, inset: linear relationship is observed in the linear scale

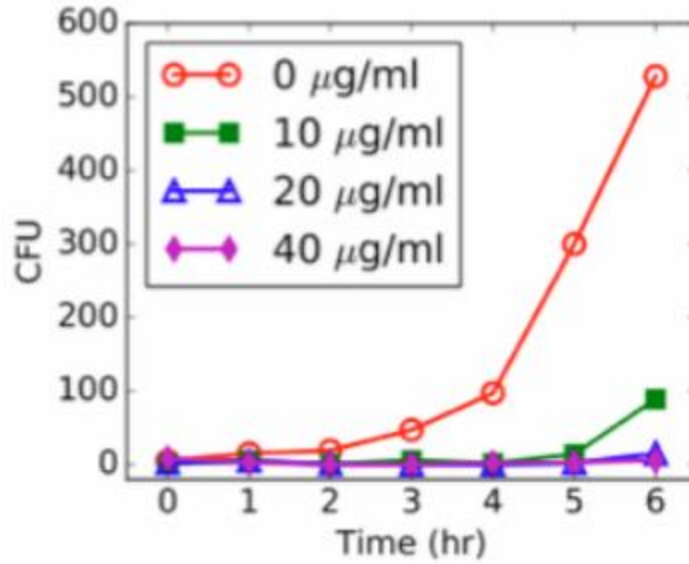


Fig. 3.4: CFU assay of *E. coli* bacteria with different concentrations of AgNPs

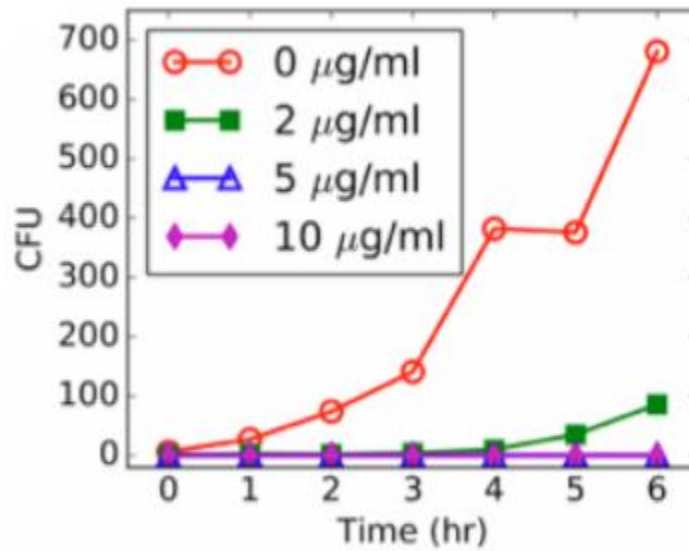


Fig. 3.5: CFU assay of *E. coli* bacteria with different concentrations of AgNO₃

One issue with the addition of AgNPs is the increase of OD₆₀₀ value and thereby opacity of the solution (Fig. 3.1 and Fig. 3.2). AgNPs exhibit high absorption and scattering of light. When light of a specific wavelength impinges on the metal surface, the conduction electrons experience a collective oscillation, which is known as Surface Plasmon Resonance (SPR) causing such high absorption and scattering of light. This property can be customized by changing the shape and size of nanoparticles. Smaller particles have absorption peaks at around 400 nm. On the contrary, larger particles show increased scattering, have broader peaks that shift towards longer wavelengths (red-shifting). Therefore, as the concentration (i.e. number of nanoparticles) increases, OD₆₀₀ will increase (Fig. 3.6) and more light will be absorbed thereby producing higher peaks (Fig. 3.7). Light absorption by AgNPs at 600 nm hampers the process of determining MIC (minimum inhibitory concentration) of *E. coli* bacteria due to two reasons:

- Determining MIC entails observing visible bacterial growth in the culture medium containing antimicrobial agents. However, addition of high concentration of AgNPs makes it difficult to observe bacteria growth separately due to high opacity caused by AgNPs.
- Addition of AgNPs of concentration ≥ 100 $\mu\text{g/mL}$ itself can produce OD₆₀₀=1.5 which is almost equal to the asymptotic value in a kinetic growth curve of *E. coli*. Therefore, running a kinetic growth curve assay of *E. coli* bacteria with AgNP of ≥ 100 $\mu\text{g/mL}$ concentration to observe the bacterial growth is impractical.

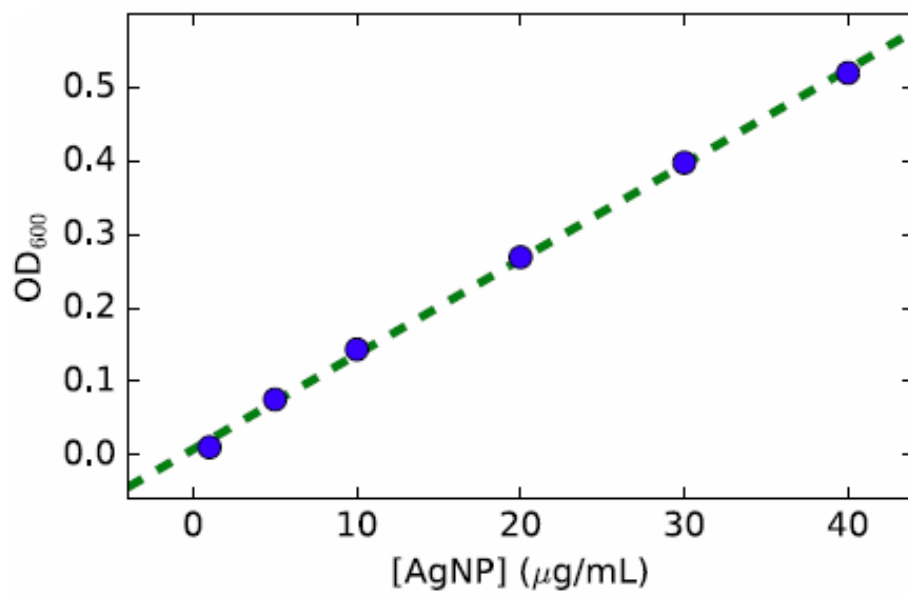


Fig. 3.6: Increase in OD₆₀₀ with the increase of AgNP concentration

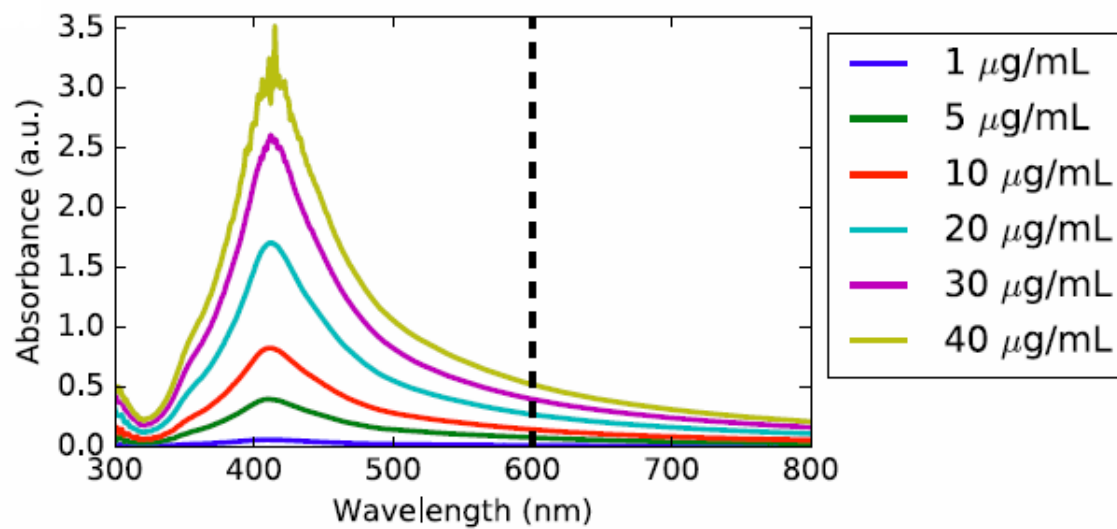


Fig. 3.7: Absorption spectra of different concentrations of AgNPs in LB medium

We have seen in the aforementioned experiments that bacteria starts to grow after 12 hours for 40 $\mu\text{g}/\text{mL}$. It proves that the MIC is beyond 40 $\mu\text{g}/\text{mL}$ in this experimental condition which agrees with the result of [70]. The OD_{600} value of the sample reached its maximum asymptotic value by 30 hours (Fig. 3.2). This value is consistent with the values for samples with lower and no concentrations of AgNPs (Fig. 3.2). It is necessary to make sure that there was no contamination. We experiments with multiple samples to make sure that all the samples provided similar results. Moreover, no bacterial growth was observed in samples containing only LB medium and only AgNPs. This ruled out any possible contamination in the experiments.

The results from the experiments with AgNPs prove that suppression by AgNPs is only temporary. To determine if the temporary suppression by AgNPs is unique, we ran kinetic growth curve assays with Ag^+ ions in the form of AgNO_3 (instead of AgNPs). Previous work showed that Ag^+ ions account for the condensation of DNA and subsequent death of cells [53]. In this work, concentrations of 0, 1, 2, 5, 7 and 10 $\mu\text{g}/\text{mL}$ were used. Antimicrobial effect of Ag^+ ions on *E. coli* bacteria was observed as shown in Fig. 3.8. For concentrations up to 10 $\mu\text{g}/\text{mL}$, bacteria were suppressed temporarily like AgNPs. Even in the case where bacteria were suppressed till 12 hours (10 $\mu\text{g}/\text{mL}$), bacteria started to grow in the second day (Fig. 3.9). However, for higher concentrations (≥ 30 $\mu\text{g}/\text{mL}$), bacteria was completely suppressed and no growth was observed up to 10 days.

An interesting similarity was observed between the kinetic growth curves of Ag^+ and AgNPs. For both cases, the suppression was observed through extension of lag times, not through decrease in maximum specific growth rate. When the suppression stage is over, bacteria starts to grow in the same growth rate for both Ag^+ (Fig. 3.9) and AgNPs (Fig. 3.2). The difference is

observable in lag time, not in their growth rate. In case of AgNPs (for 20 $\mu\text{g/mL}$ or 40 $\mu\text{g/mL}$), the initial suppression of growth is conspicuous in terms of lag time (up to 5 hours and 12 hours, respectively). But when bacteria started to grow, it grew in the same rate as the samples having lower concentrations of NPs (1, 5, 10 $\mu\text{g/mL}$) or even no NP at all. Similarly, for lower concentrations of Ag^+ ions, samples having 5 $\mu\text{g/mL}$ and 7 $\mu\text{g/mL}$ were able to stop the growth for 4 hours and 9 hours respectively. However, after the suppressed state, bacteria started to grow in the same rate as the sample having no Ag^+ ion. For quantitative analysis, the empirical growth curve was fitted with modified Gompertz model:

$$y = A \cdot \exp\left\{-\exp\left[\frac{\mu_m e}{A}(\lambda - t) + 1\right]\right\}$$

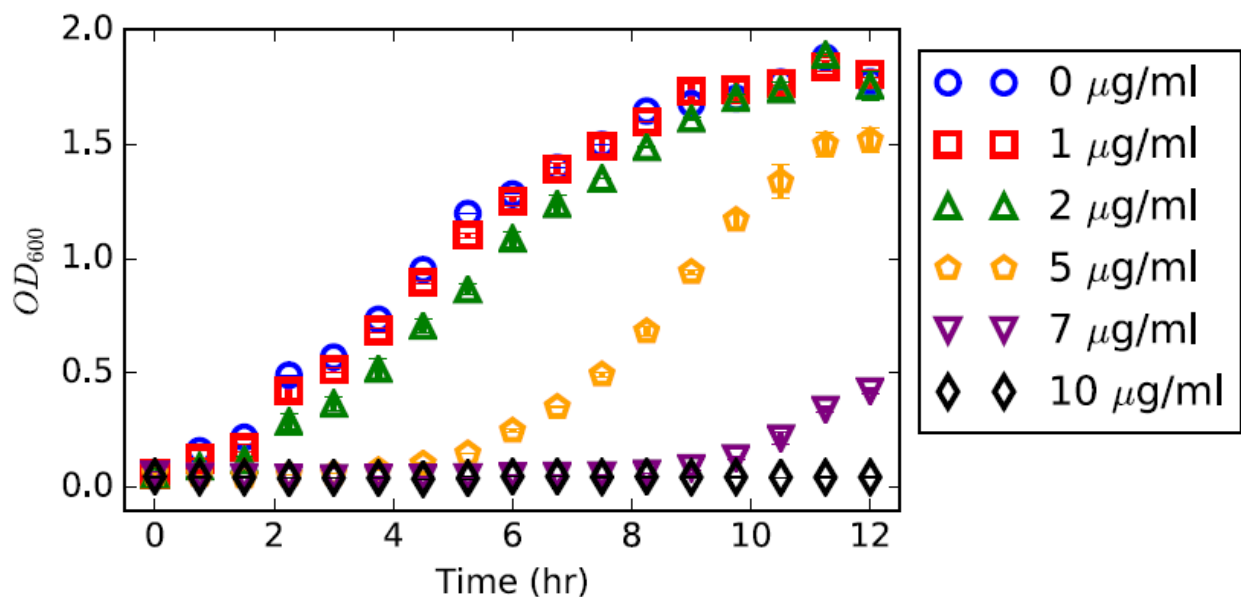


Fig. 3.8: Kinetic growth assay of *E. coli* with different concentrations of AgNO_3 (up to 12 hours)

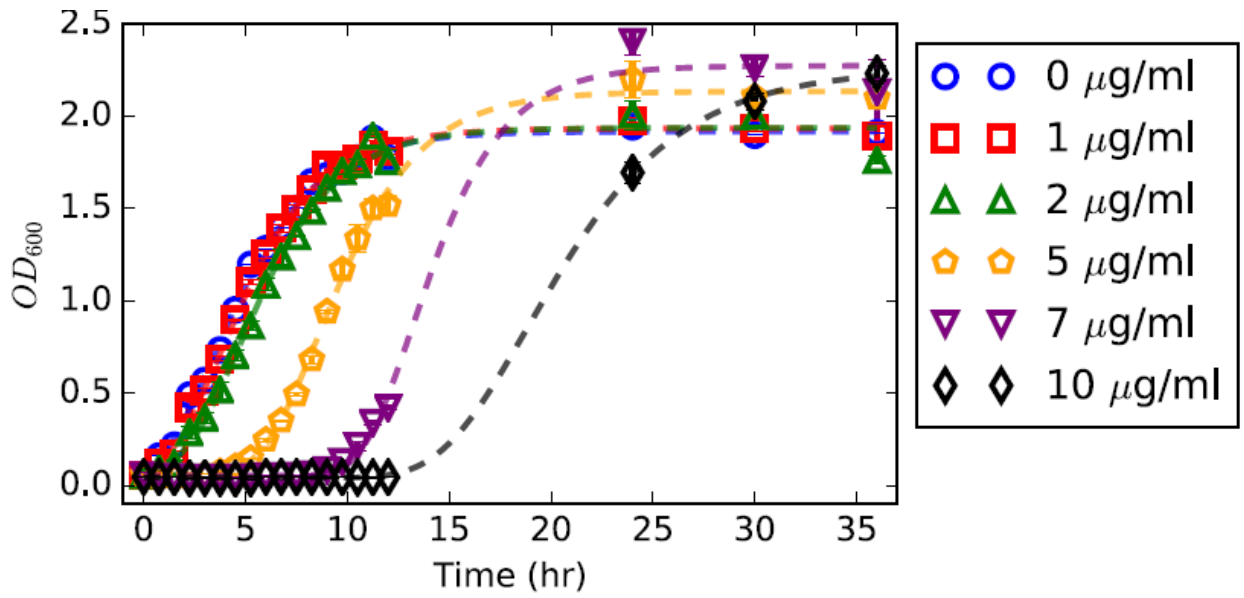


Fig. 3.9: Kinetic growth assay of *E. coli* with different concentrations of AgNO_3 (up to 36 hours, fitted with Gompertz model)

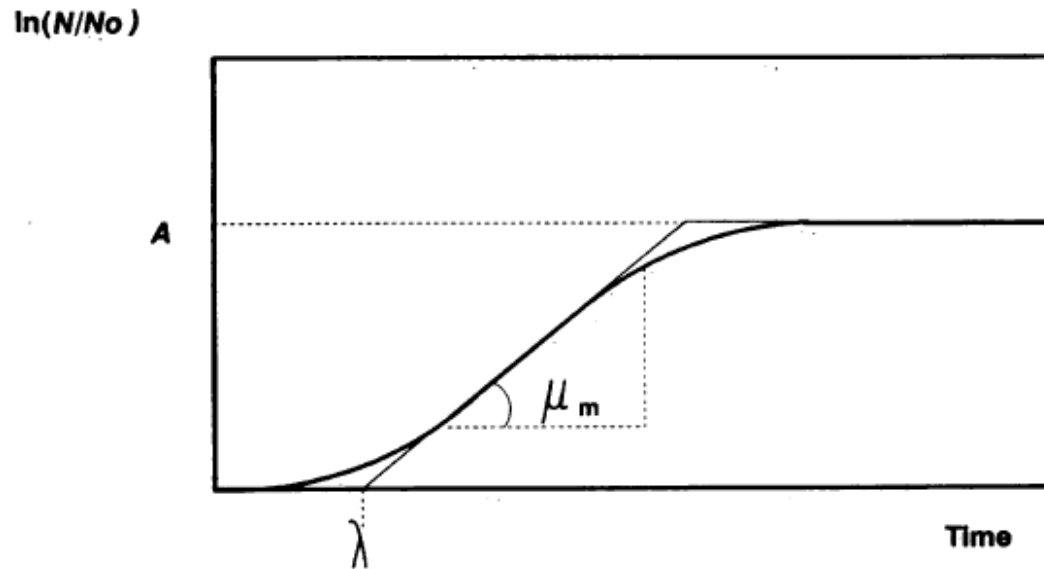


Fig. 3.10: A growth curve [71]

Mathematical models can be used to assume how microorganism may behave at different conditions like pH, temperature, presence of water etc [71]. Since they can predict the behavior of bacteria, modeling of bacterial growth is an important field of study [71]. To build a mathematical model, bacterial growth needs to be recorded and analyzed [71]. There are different parameters that are normally considered while forming a mathematical model[71]. When the graph is plotted as log (number of organisms) vs time, it takes a sigmoidal shape [71]. Bacterial growth rate starts from zero and then quickly reaches to a maximum value (maximum specific growth rate, μ_m) [71]. In practice, this is determined by calculating the slope of the most linear part of the growth curve [71]. The asymptote of μ_m intersects the x-axis at a specific positive value [71]. This is defined as the lag time, λ [71]. Therefore, in a time dependent growth curve, lag time corresponds to a time length when bacteria start to show maximum growth rate [71]. After this, bacterial growth rate starts decreasing until the growth reaches a maximum value [71]. This maximum value at this stage is denoted as the Asymptote (A) [71]. The region right after $t=\lambda$ is the exponential phase followed by a stationary phase [71].

A number of models have been developed over time such as: Gompertz [72], Richard [73], Schnute [74] etc. Among these models, Schnute model entails all the features of other models and can be considered as a comprehensive model [71]. By determining specific parameters and 95% confidence intervals, the most suitable model can be chosen [71]. Although all the models provide reasonably good fitting, Schnute model and Richard model face overflow problems at times [71]. However, Gompertz model never exhibits such problem [71]. Therefore, Gompertz model is the mostly accepted model of all based on 95% confidence limit and Student t test [71]. Gompertz model provides satisfactory results for *L. Plantarum*, *Pseudomonas putida*, *Staphylococcus aureus*, *Candida parapsilosis* etc. [71].

Due to the widely accepted feature of Gompertz model, it was used to fit data derived from kinetic growth curve experiments. From the fitting, growth rate (μ) and lag time (λ) parameters were extracted and plotted against the concentrations of AgNPs and AgNO₃ (Fig. 3.11-Fig. 3.14). From Fig. 3.11-Fig. 3.12, it was observed that growth rates were similar (within error) irrespective of the concentrations for both AgNPs and AgNO₃. On the other hand, significant rise in lag time (λ) with increasing concentration was observed for both AgNPs and AgNO₃ (Fig. 3.13-Fig. 3.14). This dose dependence of lag time can be fitted well with quadratic functions.

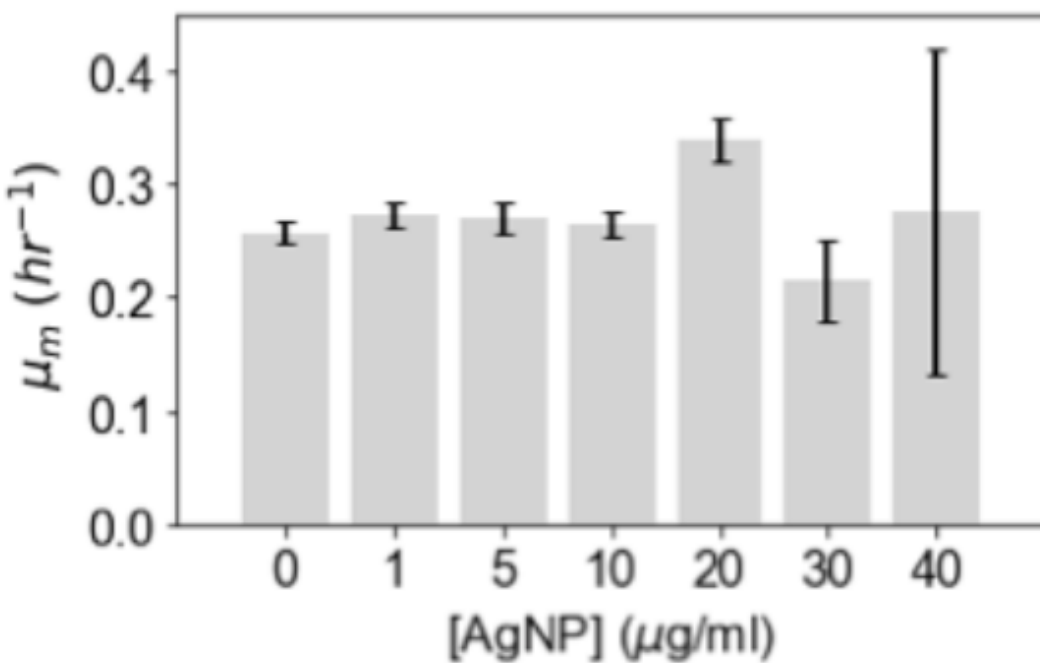


Fig. 3.11: Relation between maximum specific growth rate (μ_m) and concentration of AgNP

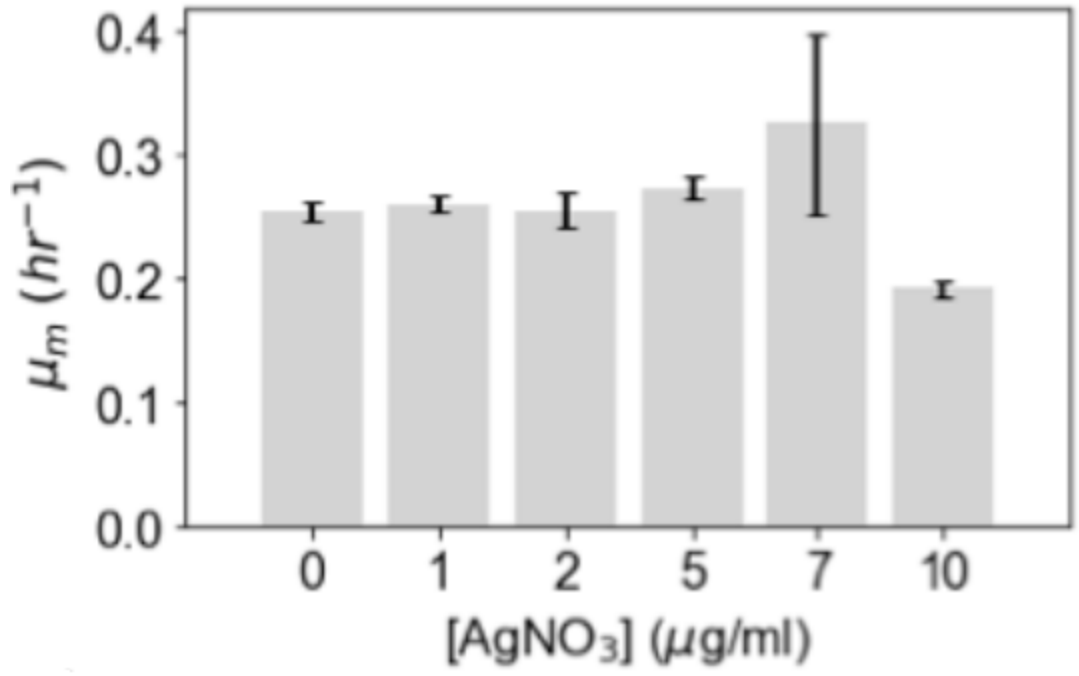


Fig. 3.12: Relation between maximum specific growth rate (μ_m) and concentration of AgNO_3

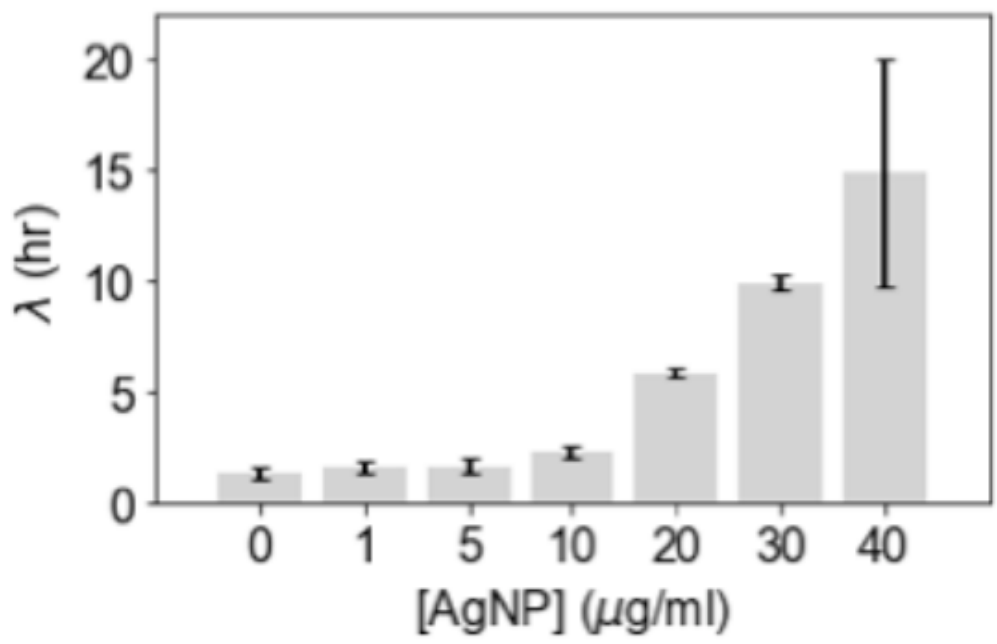


Fig. 3.13: Relation between lag time (λ) and concentration of AgNP

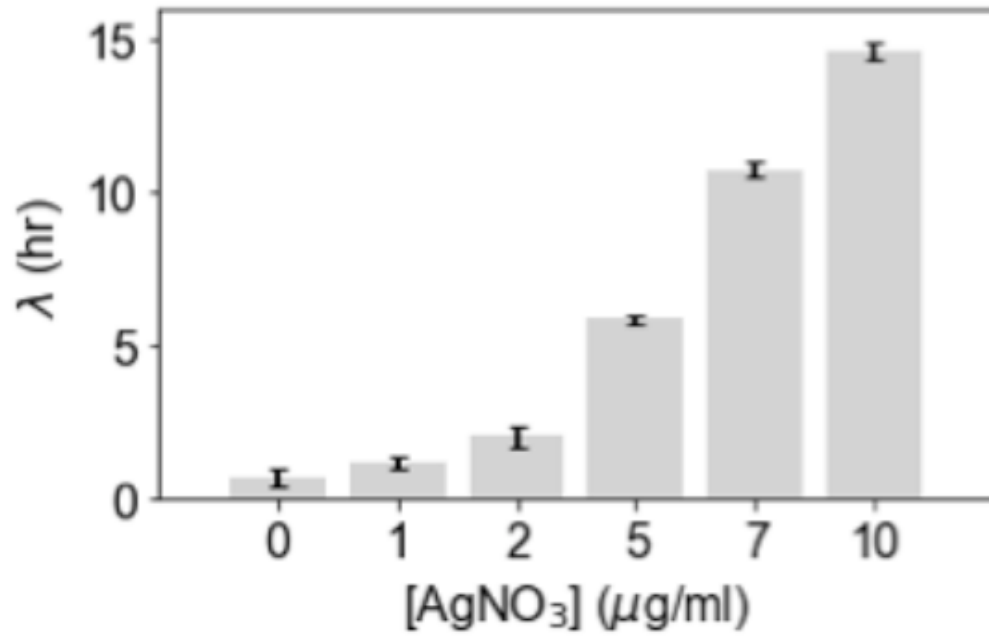


Fig. 3.14: Relation between lag time (λ) and concentration of AgNO_3

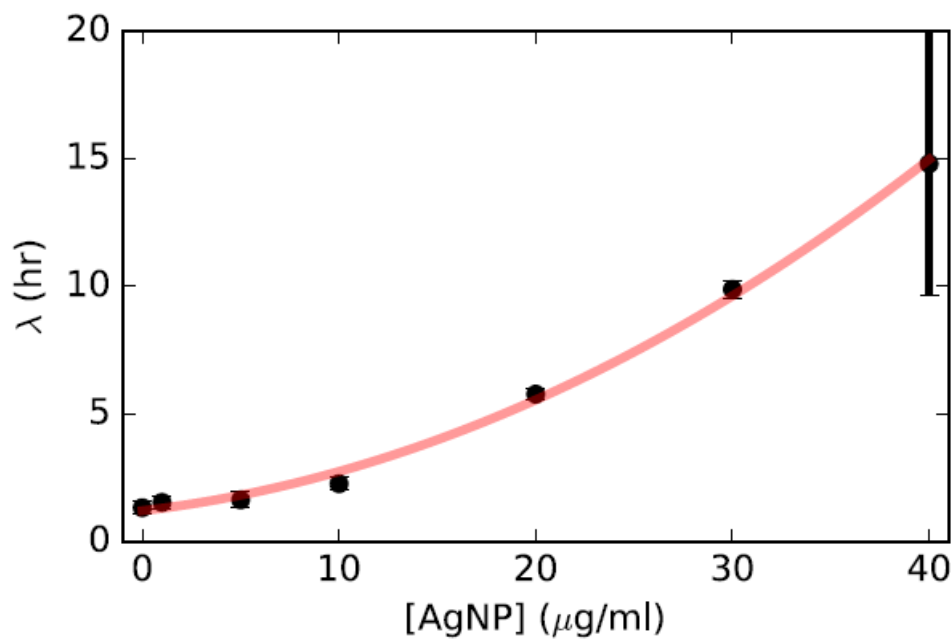


Fig. 3.15: Parabolic dependence of lag time (λ) on concentration of AgNP

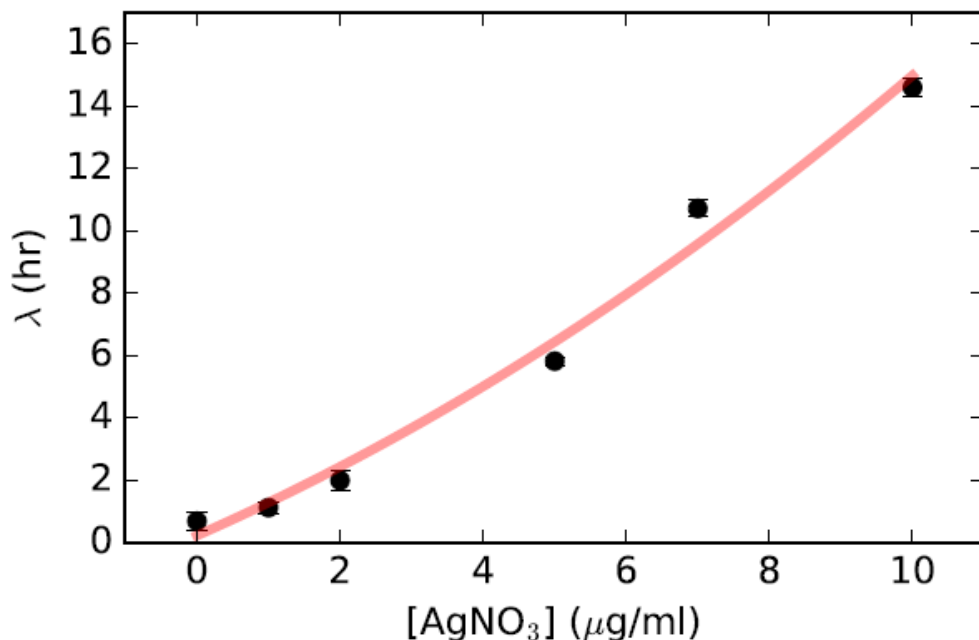


Fig. 3.16: Parabolic dependence of lag time (λ) on concentration of AgNO_3

Previous work on the effect of antibiotics over bacteria can be found in literature [75]. It was found that increase in antibiotic concentration reduces growth rate, but lag time is barely affected [75]. Therefore, based on the difference between previous work on antibiotics and this study on AgNPs and Ag^+ ion, it can be reported that that antimicrobial property of AgNP is somewhat different from traditional antibiotics.

3.2 Time-kill curves:

To find out if bacteria were actually killed by AgNPs or Ag^+ ions, time-kill curves were produced using CFU assay. For the CFU assay, samples containing bacteria treated with different concentrations of AgNPs (0, 10, 20, 40, 80 $\mu\text{g/mL}$) and Ag^+ ions (5 $\mu\text{g/mL}$) were plated on LB agar plates and incubated overnight. The number of colony counts is directly proportional to the number of live cells in the sample. In Fig. 3.17, number of bacteria colonies reduced for

first few hours due to the presence of Ag^+ ions ($5 \mu\text{g/mL}$) and AgNPs ($20 \mu\text{g/mL}$). For $5 \mu\text{g/mL}$ Ag^+ ions, number of colonies reduced from 100 to 0 in 3 hours. It indicated the death of more than 99% of bacteria cells. On the other hand, for $20 \mu\text{g/mL}$ AgNPs, around 67% of bacteria cells were killed before bacteria started to grow again. Nevertheless, both Ag^+ ions and AgNPs were able to kill a fraction of *E. coli* bacteria.

From Fig. 3.17, it can be said that killing of bacteria follows an apparently straight line for both Ag^+ ions and AgNPs. Therefore, killing by AgNPs or Ag^+ ions can be explained by a simple differential equation:

$$\frac{dn}{dt} = -\alpha \cdot n(t) \text{ or}$$

$$n(t) \sim e^{-\alpha t}$$

Where, α represents the killing rate by the antimicrobial agent.

Moreover, from Fig. 3.17, it appears that killing rate of Ag^+ ion is higher than AgNPs since the number of colonies decreases more rapidly than AgNPs. A possible reason might be that AgNPs first need to release Ag^+ ions before killing thereby taking more time to start killing bacteria since AgNP alone does not show any toxicity towards *E. coli* without releasing Ag^+ ion [41].

The dependence of bacteria killing kinetics on the concentration of AgNPs can also be analyzed using time-kill curves of Fig. 3.18. Here CFU assays were performed for *E. coli* treated with different concentrations of AgNPs (0, 10, 20, 40, 80 $\mu\text{g/mL}$). It can be observed that larger number of cells were killed in presence of higher concentration of AgNPs before bacteria started to regrow (Fig. 3.18). Besides, the time from addition of AgNPs to the point where bacteria

started to regrow (i.e. effective killing time) also increases with the increase in concentration of AgNPs (Fig. 3.18). However, the killings rate look similar for all the concentrations used (Fig. 3.18).

From Fig. 3.4, Fig. 3.5 and Fig. 3.18, it is quite clear that exponential growth phase shifts right in presence of AgNPs. Therefore, the time it takes for the bacteria to be prepared for growing exponentially gets longer with the addition of AgNPs compared to the case where no AgNP was added. In other words, the lag times increased with the increase of AgNP concentrations which complies with the observation from kinetic growth assays.

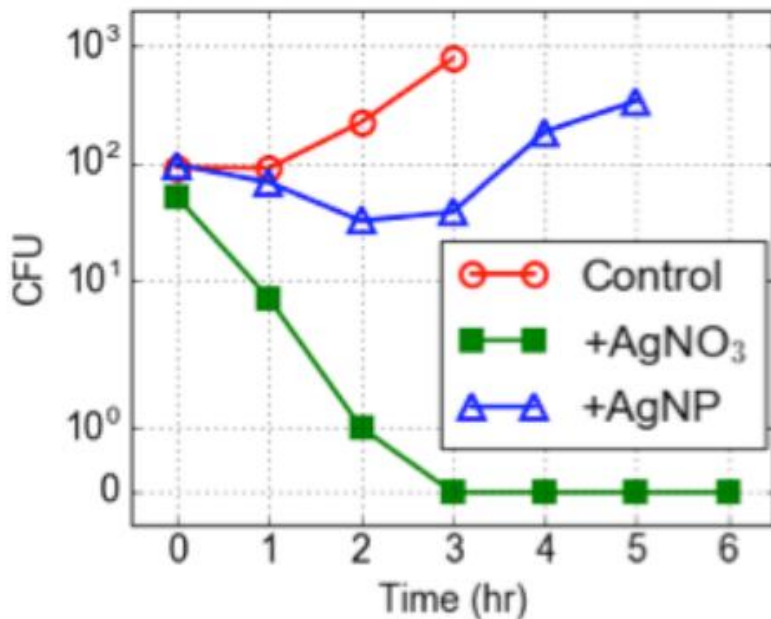


Fig. 3.17: Time-kill curve for *E. coli* bacteria in LB medium without Ag (red circles), 5 $\mu\text{g/mL}$ AgNO₃ (green squares), 20 $\mu\text{g/mL}$ AgNPs (blue triangles)

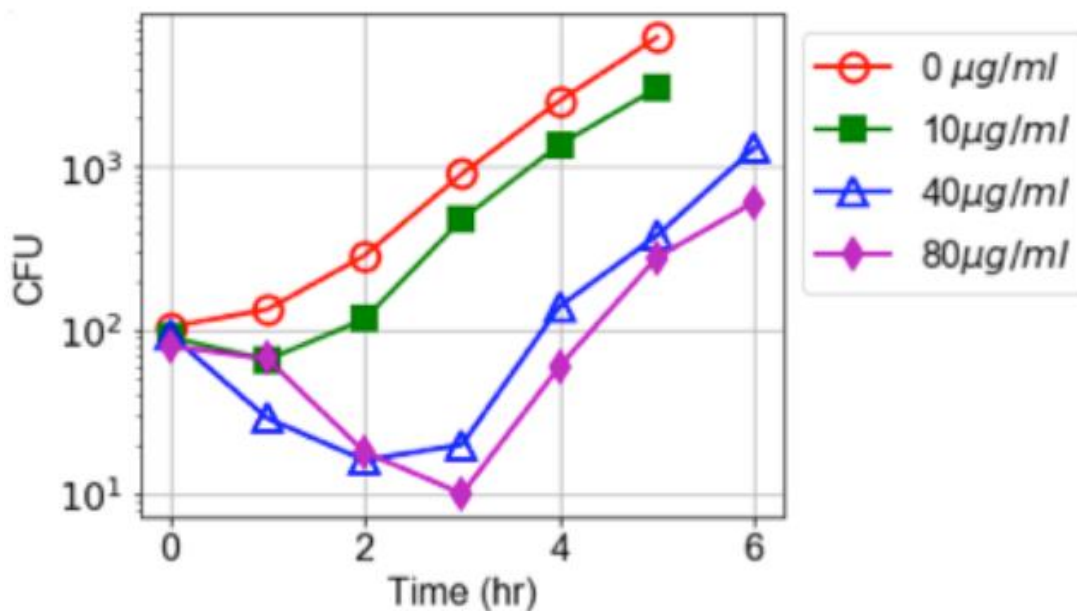


Fig. 3.18: Time-kill curves for *E. coli* bacteria in LB medium against different concentrations of AgNPs

So far the growth curves discussed were generated for AgNPs and Ag^+ ions added in the lag phase (with an initial $\text{OD}_{600}=0.05$ of bacteria). To see whether they can suppress the growth when bacteria is already in the exponential phase, kinetic growth assays were performed by adding AgNPs to the *E. coli* culture after the OD_{600} value of bacteria reached ~ 0.5 . Due to high absorption of light by AgNPs (Fig. 3.6 and Fig. 3.7), sudden jumps in OD_{600} readings were recorded as seen in Fig. 3.19. However, change in bacteria growth can be observed as the slopes get gentler. By subtracting the OD_{600} values generated by only AgNPs from the overall OD_{600} values, the change in bacteria growth becomes quite clear. In Fig. 3.21, the decrease in bacteria growth is observable after the addition of AgNPs in the exponential phase. Similar results were observed after the addition of AgNO_3 in the exponential phase of bacteria growth. The change in OD_{600} values is seen in Fig. 3.20 whereas halted growth in the exponential phase is evident in Fig. 3.22 after subtracting the contribution by AgNO_3 to OD_{600} readings.

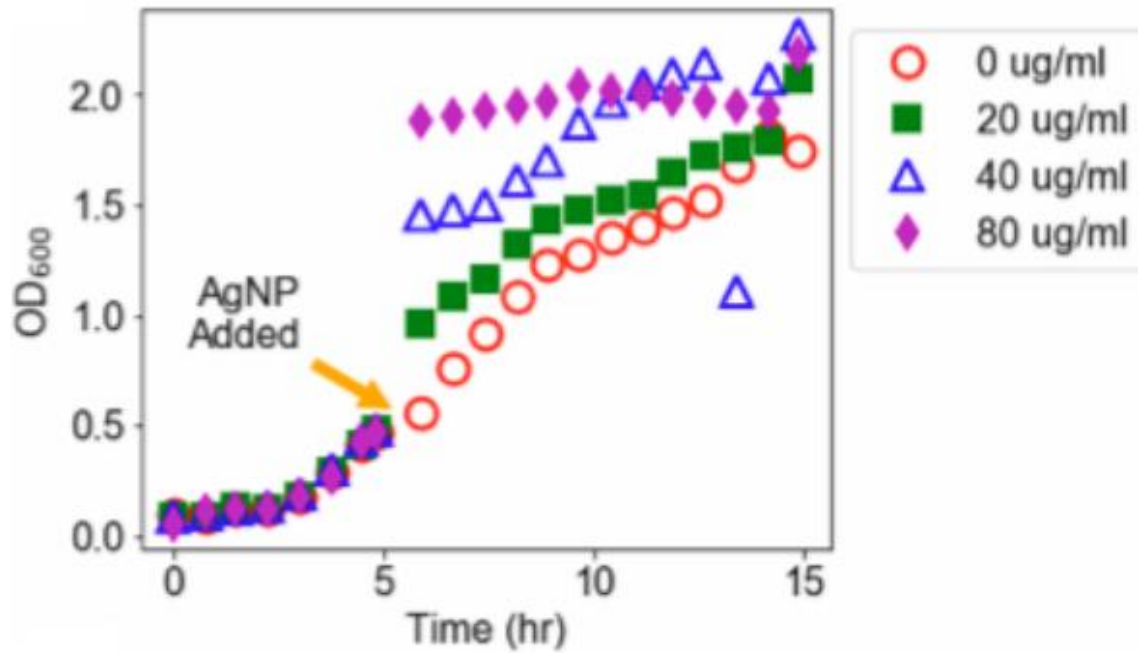


Fig. 3.19: Change in OD₆₀₀ readings after the addition of AgNPs in exponential phase

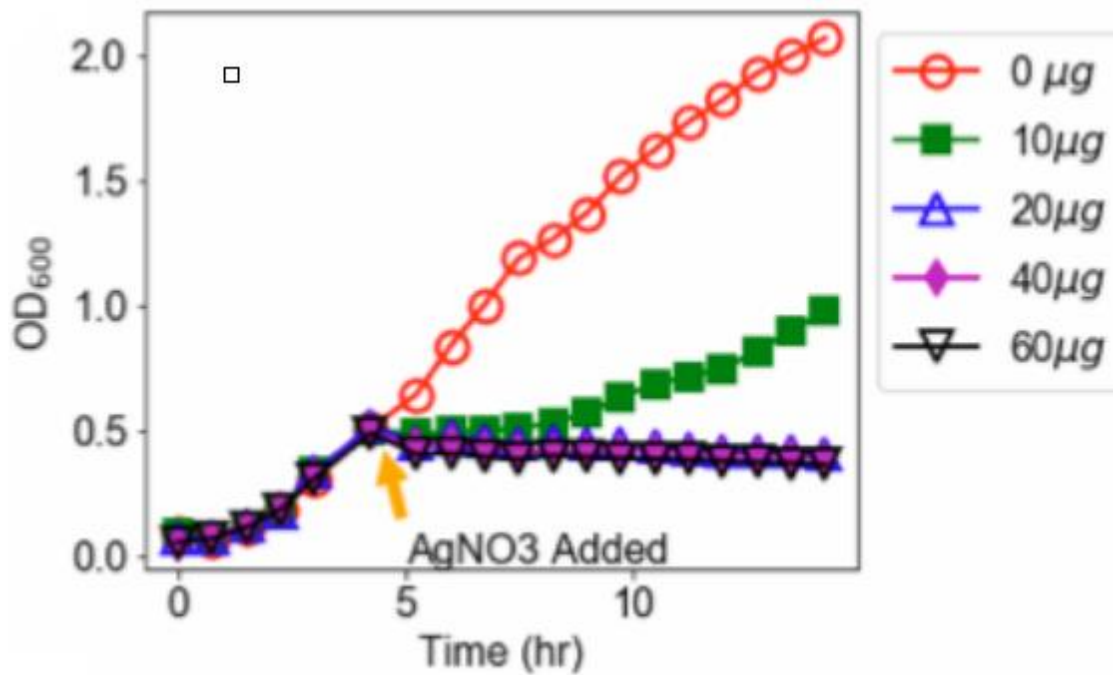


Fig. 3.20: Change in OD₆₀₀ readings after the addition of AgNO₃ in exponential phase

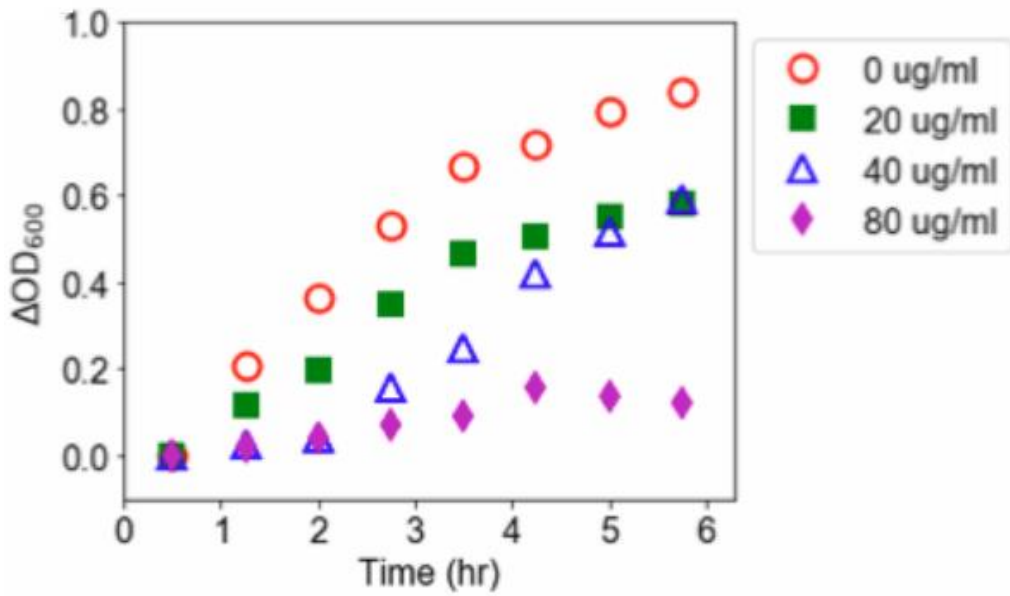


Fig. 3.21: Halted growth of bacteria after the addition of AgNPs in exponential phase

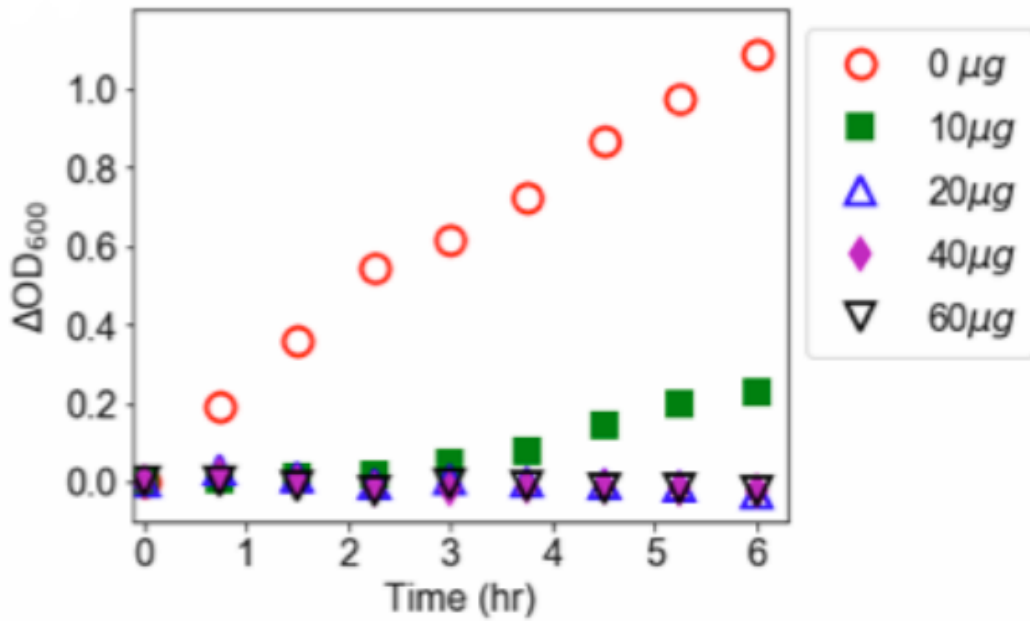


Fig. 3.22: Halted growth of bacteria after the addition of AgNO₃ in exponential phase

One observation from time-kill curves and kinetic growth assays is that addition of AgNPs or Ag⁺ ions causes little decrease in kinetic growth assays whereas number of colonies in CFU assays drops significantly. This is because of the difference in outcomes of these methods. In the CFU assays, only the live cells grow into colonies whereas OD₆₀₀ reading by NanoPhotometer considers all cells that are not lysed. The OD₆₀₀ reading by NanoPhotometer cannot distinguish between alive and dead cells. Therefore, this observation indirectly suggests that killed cells by AgNPs or Ag⁺ ions were most likely not lysed, but dead only. This result is also consistent to a model by Zhou et al. [31] and works using TEM imaging and X-ray microanalysis [53], [76].

CHAPTER FOUR

Quantitative Model and Verification

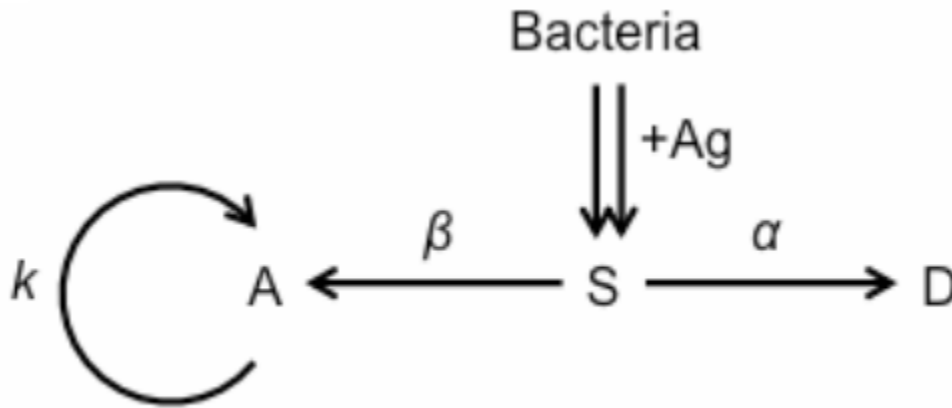


Fig. 4.1: Schematic representation of the proposed SAD model

4.1 Proposed Quantitative model:

A quantitative model has been proposed based on the experimental results to explain the antimicrobial properties of Ag^+ ions and AgNPs. The model should satisfy the experimental observations from kinetic growth assays, CFU assays and time-kill curves. Followings are the conspicuous experimental findings:

- I. Presence of AgNP slowed down the bacterial growth by extending the lag time (λ)
- II. Despite the increase in lag time, maximum growth rate (μ_m) was not affected by the addition of AgNPs.

- III. AgNPs killed some *E. coli* bacteria cells. Although the killing rate was somewhat independent of AgNP concentration, survival percentage dropped with the increase of AgNP concentration.
- IV. AgNP can partially or completely stop the bacterial growth in the exponential phase.

The developed model is shown in the Fig. 4.1. When Ag is added in the form of either AgNP or Ag⁺ ions, bacteria is pushed to the suppressed state, S. As a result, bacteria experienced two potential states:

- 01. Some of them get killed thereby moving to the dead state (D)
- 02. Others take some time to adapt to the surroundings and then get back to the active state (A). In the active state, they grow and reproduce normally like untreated cells.

This model has been termed as Suppressed-Active-Dead (SAD) model. Bacterial cell number as a function of time $n(t)$ can be a starting point to go through the model [77]. At any moment, the growth of bacteria can be described by the differential equation,

$$\frac{dn(t)}{dt} = k \cdot n(t)$$

Where, k is the specific growth rate and it depends on the surroundings [77]. If the growth medium of bacteria is unlimited, bacteria growth is exponential and surrounding conditions remain unchanged [77]. Therefore, k remains unchanged and can be expressed as

$$k = k_0 = \text{constant}$$

However, if the growth medium is limited, bacteria have to fight for available resources as the number of cells increase [77]. Let the initial available resource be 1. As the population increases, the growth rate will become

$$k = k_0 \left(1 - \frac{n}{A}\right)$$

Where, k_0 is the initial growth rate and A is asymptotic cell density [77]. It is noticeable that, growth rate becomes zero when $n=A$ [77]. It gives the equation for the bacterial growth as

$$\frac{dn(t)}{dt} = k_0 \left(1 - \frac{n(t)}{A}\right) \cdot n(t)$$

Solving the differential equation gives the bacterial growth curve equation:

$$n(t) = \frac{A}{1 + \left(\frac{A - n_0}{n_0}\right) \cdot e^{-k_0 t}} \quad (1)$$

At $t=0$, cell number is n_0 .

At $t=\infty$, cell number reaches the asymptotic value A [77]. Depending on how k is defined, different models can be formulated [77].

Optical Density (OD_{600}) of the sample corresponds to the cell number in the sample. Therefore, same equation applies for both OD_{600} value of the bacteria culture and the cell density [78].

The proposed model entails the transitions from one stage to the other ($S \rightarrow A$ and $S \rightarrow D$). Thus three sets of differential equations altogether represent the SAD model:

$$\left. \begin{aligned} \frac{dn_a}{dt} &= +\beta n_s + k_0 \left(1 - \frac{n_a}{A - n_d - n_s} \right) n_a \\ \frac{dn_s}{dt} &= -\alpha n_s - \beta n_s \\ \frac{dn_d}{dt} &= +\alpha n_s \end{aligned} \right\} \quad (2)$$

Where, α = killing rate when bacteria are transforming from the suppressed state to the dead state and β = wake-up rate for the bacteria while shifting from suppressed state to active state.

4.2 Application in experimental condition for Verification

After the SAD model was numerically solved, it was found that the predictions from the SAD model matched with the key observations in the aforementioned experiments. Using this model, different growth curves have been plotted in Fig. 4.2. These plots have the same killing rate α but varying wake-up rate β . Since all the cells, dead or alive, contribute to the OD₆₀₀ values, all bacteria cells ($n_{OD} = n_a + n_s + n_d$) were considered for plotting. It has been assumed that the dead cells have not been lysed in the entire process. Moreover, the shape of the growth curves were also similar (sigmoid) to the logistic growth (blue curve in Fig. 4.2 and Eq. 1) of the ‘wild type sample’ (sample where bacteria are grown without the presence of any potential suppressive component, for example Ag⁺, AgNPs etc.).

Logistic growth represents the bacterial growth when resources are limited and each individual has to fight for existence. Therefore, it provides the maximum final population that a limited environment can sustain. Exponential regions of the growth curves corresponding to different wake-up rates were parallel to each other and the ‘wild type’ sample. It proves that the maximum growth rates μ_m were not affected by either the addition of the suppressed state or the wake-up

rate, β . On the other hand, the lag time extension for smaller wake-up rates was easily observable, which was apparently due to higher concentrations of Ag.

Time-kill curves were generated using the SAD model where live bacterial cell population (both active and suppressed, $n_{CFU}=n_a+n_s$) were plotted against time with different wake-up rates. This model replicated the time-kill curves generated experimentally from the CFU assay as shown in Fig. 4.3. In the time-kill curves using the SAD model, the number of bacteria colonies first decreased and then rose again in the similar manner as we saw in the time-kill curves using CFU assay. Besides, the threshold point moves lower in the upright direction corresponding to longer killing time and smaller wake-up rates. This also matches with the use of higher concentration of Ag in the experimental time-kill curves.

The experimental results show that introduction of AgNPs or Ag^+ in the exponential phase of bacterial growth interrupts the growth. This phenomenon can also be predicted from the SAD model. For this, the bacteria population was first estimated considering the initial condition that all the bacteria were in the active state. When the OD_{600} value reached 0.5, Ag was added thereby virtually pushing all the cells to the suppressed state. After this, bacteria cell density ($n_{OD} = n_a + n_s + n_d$) was determined as a function of time according to the SAD model. The results accurately predicted the suppression of bacteria as we can see in Fig. 4.4: smaller wake-up rates (i.e. higher Ag concentration) slowing bacterial growth. We can see from Fig. 3.19-Fig. 3.22 how well the interpretations from the model matches with the experimental results.

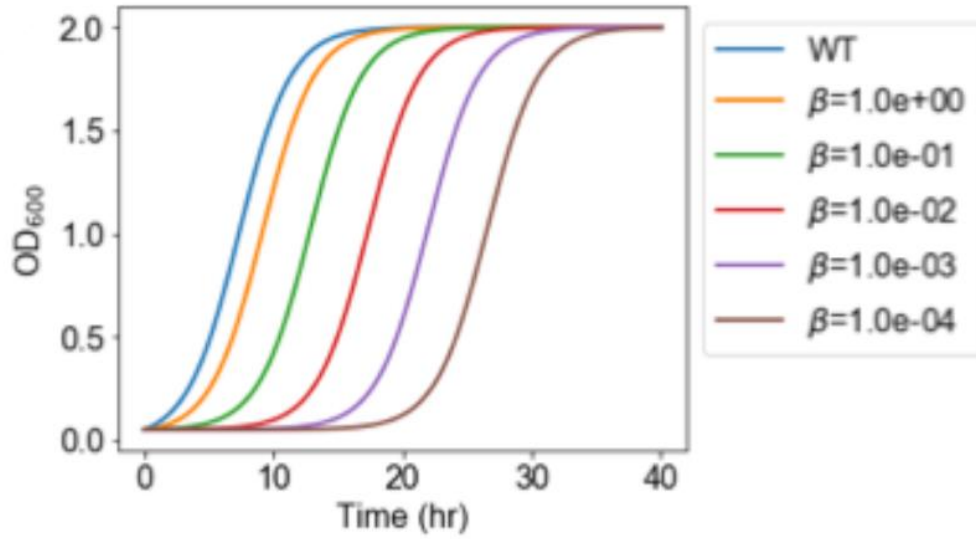


Fig. 4.2: Simulated kinetic growth curves of *E. coli* bacteria using SAD model ($\alpha=0.71$)

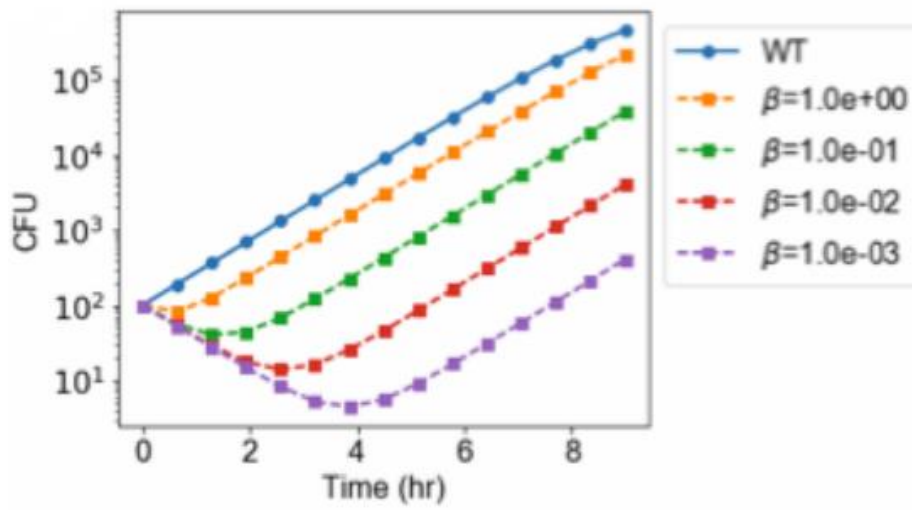


Fig. 4.3: Simulated CFU count using the SAD model ($\alpha=0.71$)

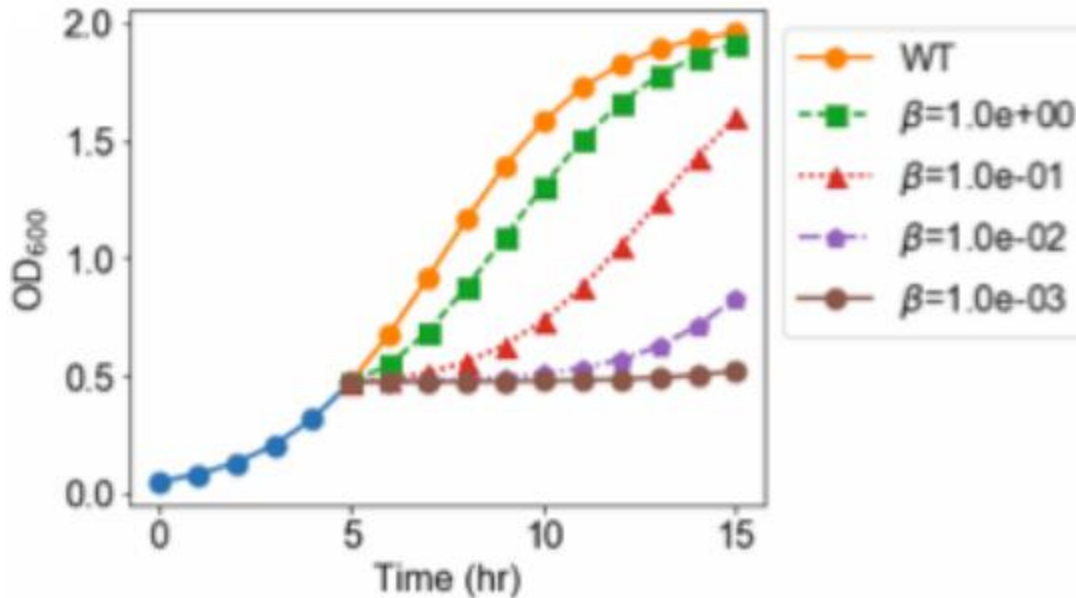


Fig. 4.4: Simulated growth curves of *E. coli* bacteria in the exponential phase using the SAD model ($\alpha = 0.71$)

One significant point of the proposed model is that it can explain both bacteriostatic and bactericidal properties of antimicrobial elements. However, the real definitions of ‘bacteriostatic’ or ‘bactericidal’ are somewhat arbitrary [79]. Strictly speaking, bacteriostatic agents are supposed to inhibit the growth of bacteria in a stationary phase, not entirely kill them [79]. On the other hand, bactericidal agents are supposed to kill the bacteria entirely [79]. Nevertheless, in reality, bactericidal agents cannot kill every bacterium within 18-24 hours of the test whereas bacteriostatic agents kill some bacteria within that period [79]. Bacteriostatic agents can even kill up to 90%-99% of bacteria, but to be called as bactericidal, they have to kill at least 99.9% of them [79]. Besides, bacteriostatic or bactericidal properties also vary depending on growth conditions, bacterial concentration and time length of test [79]. The proposed model can anticipate bacteriostatic or bactericidal properties based on two parameters, α and β . A high α

value indicates a possible bactericidal effect whereas a high β value emphasizes the existence of bacteriostatic effect.

SAD model can be extended to formulate more complicated models and can be used to explain the behavior of persisters. Persisters are fractional quiescent bacterial cells that can survive exposure to bactericidal drugs and are able to revive under specific conditions [80]. The number of persisters depends on the culture medium, type of antibiotic agent, exposure time, antibiotic concentration etc. [80]. It means that persisters surviving in one condition may not survive in another condition [80]. Models have been proposed before to explain the heterogeneous mechanism of persisters [80]. The SAD model can also be extended to explain persisters' mechanism alongside using as an effective model for bactericidal or bacteriostatic agents.

4.3 Parameter extraction and Application

In the quantitative model, the antimicrobial activity is determined by two parameters: α (the killing rate) and β (the wake-up rate). These parameters can be extracted using the experimental results. Bacteria killing was observed in the initial portion of the time killing curves (before the threshold points where bacteria have not started growing) derived from CFU assays. Therefore, this portion can be used to determine the value of α . Up to 80 $\mu\text{g/mL}$ of concentrations have been used and the killing rate was found to be independent of the concentration of AgNPs (Fig. 3.18). Consequently, a single line was enough to be fitted for different concentrations of AgNPs with the initial portion of the time killing curves (Fig. 4.5 and Fig. 4.6). It was found that $\alpha = 0.71 \pm 0.03 \text{ hr}^{-1}$ (Fig. 4.6). The value of α (i.e. killing rate) for Ag^+ ions was apparently larger than AgNPs.

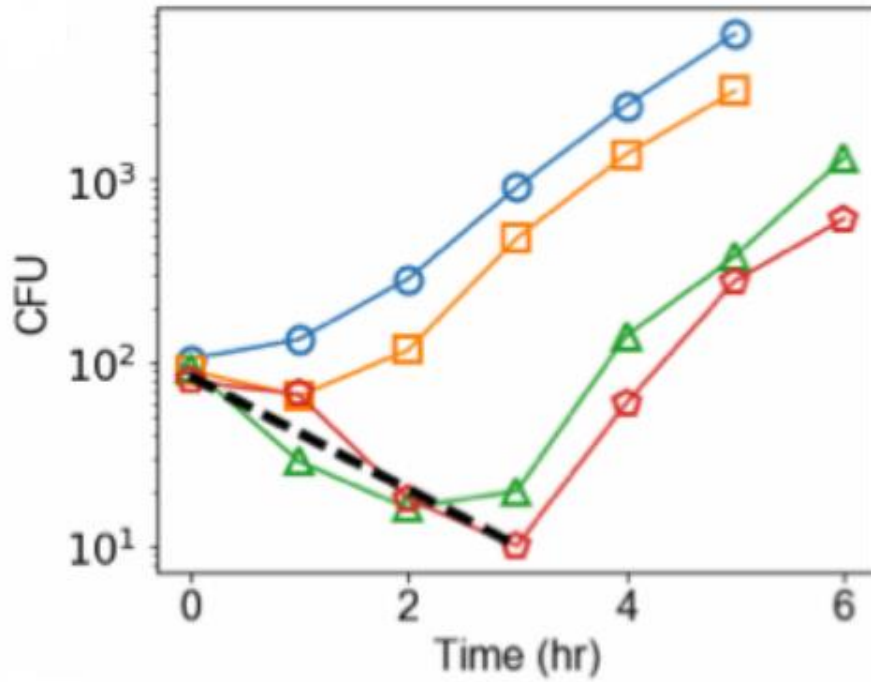


Fig. 4.5: Use of empirical time-kill curves to determine killing rate, α

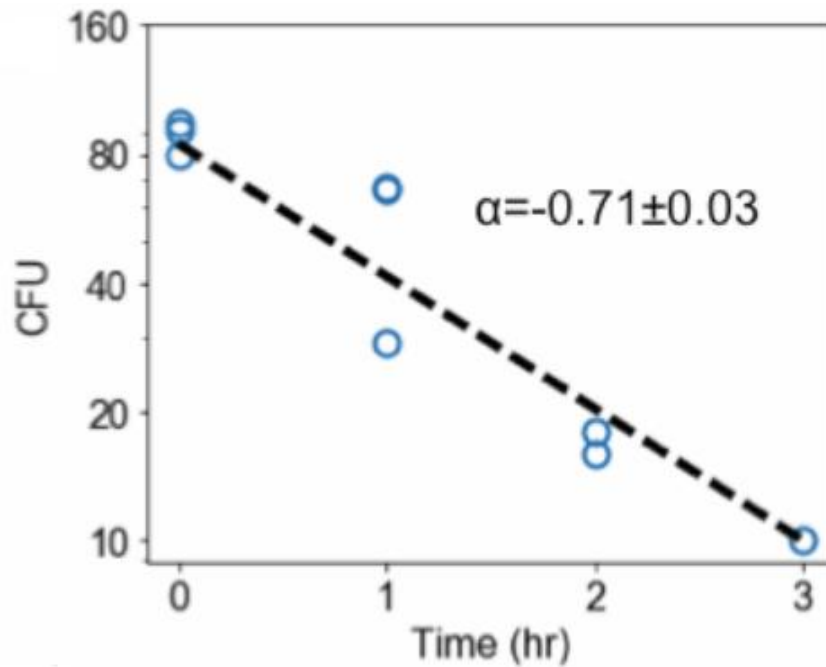


Fig. 4.6: Magnified view of Fig. 4.9 to show the data points used for fitting

Using the value of the killing rate α , the value of wake-up rate β can be determined. The plan is to optimize β for the model with the derived value of $\alpha=0.71$ so that growth curves plotted from the model (Eqns. 2) overlay the experimental kinetic growth curves (Fig. 3.1, Fig. 3.2, Fig. 3.8, Fig. 3.9). This process is similar to curve fitting through numerical least-square regression method. The main objective of this method is to achieve minimal value of the squared residuals

$$S = \sum_{i=1}^n (y_i - y_i^*)^2$$

Where, y_i are the measured values and

$y_i^* = f(x_i, \beta)$ are the fitted values.

However, while calculating the value of $y_i^* = f(x_i, \beta)$, instead of using an explicit function $f(x_i, \beta)$, the model in Eqns. 2 were solved to obtain the fitted y values in least square curve fitting. Moreover, by determining different β values from different kinetic growth curves of *E. coli* for different concentrations of AgNPs, the relation between wake-up rate β and concentration of AgNPs in the growth media can be obtained. However, while fitting the growth curves to determine β , no information regarding the concentration of AgNPs was required. It proves that although determination of β does not explicitly depend on the concentrations of AgNPs, these two are strongly correlated with each other. We can see this on Fig. 4.7 where logarithm of wake-up rate β is linearly related to the concentration of AgNPs. Representing the straight line with the equation $\ln\beta = \kappa_s \cdot [AgNP] + \theta_s$ (where $[AgNP]$ means the concentration of AgNPs) and fitting with $\ln\beta - [AgNP]$ plot gives $\kappa_s = -0.39 \pm 0.03$ and $\theta_s = 4.2 \pm 0.8$. The negative slope in Fig. 4.7 indicates that higher concentrations of AgNPs would result longer lag phases which concurs with the experimental observation (Fig. 4.13-Fig. 4.16).

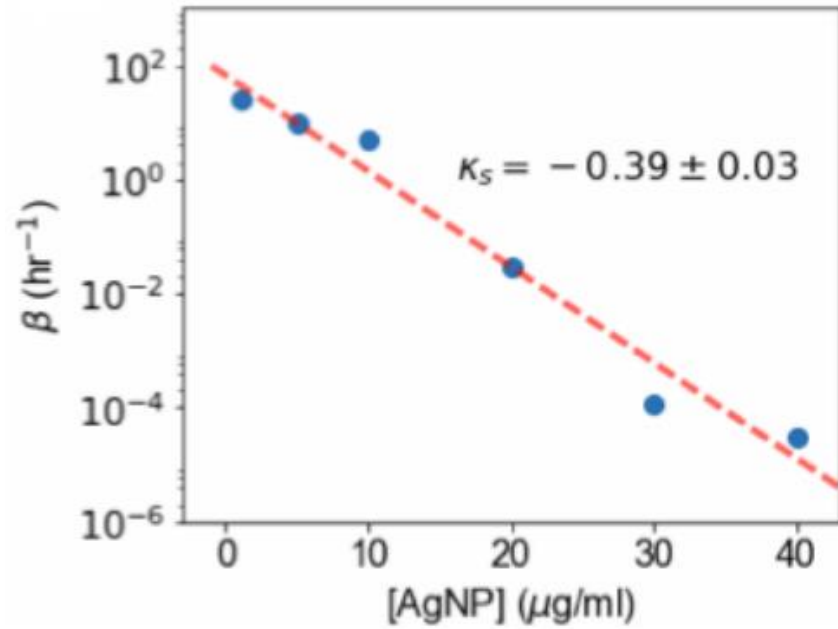


Fig. 4.7: Relation between wake-up rate β and AgNP concentration

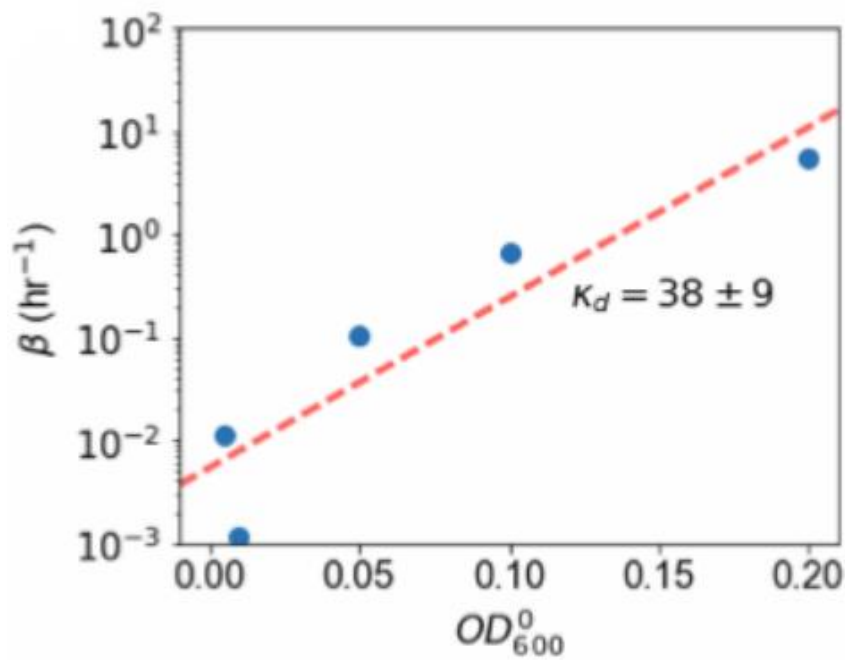


Fig. 4.8: Relation between wake-up rate β and initial concentration of bacteria when AgNPs were added

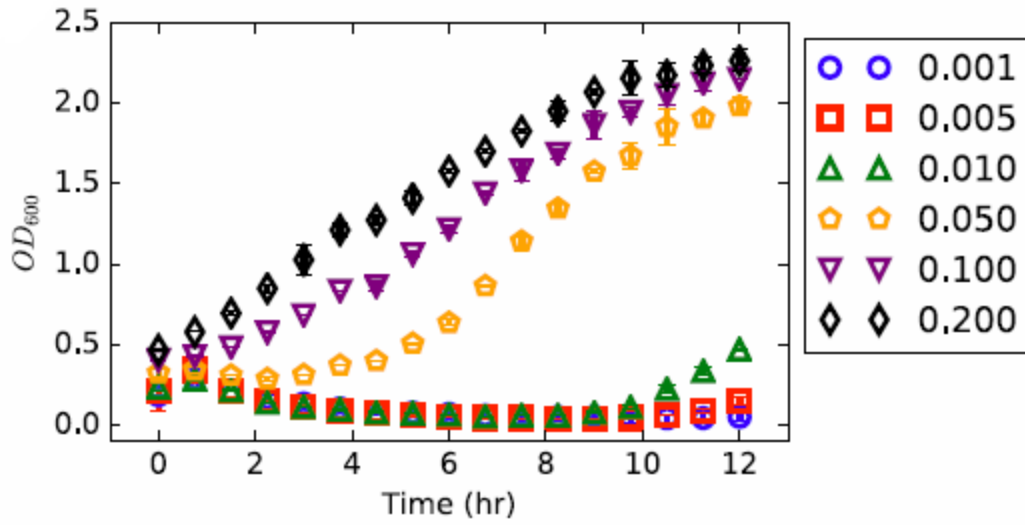


Fig. 4.9: Suppression of bacteria (with different initial concentrations) by AgNPs up to 12 hours

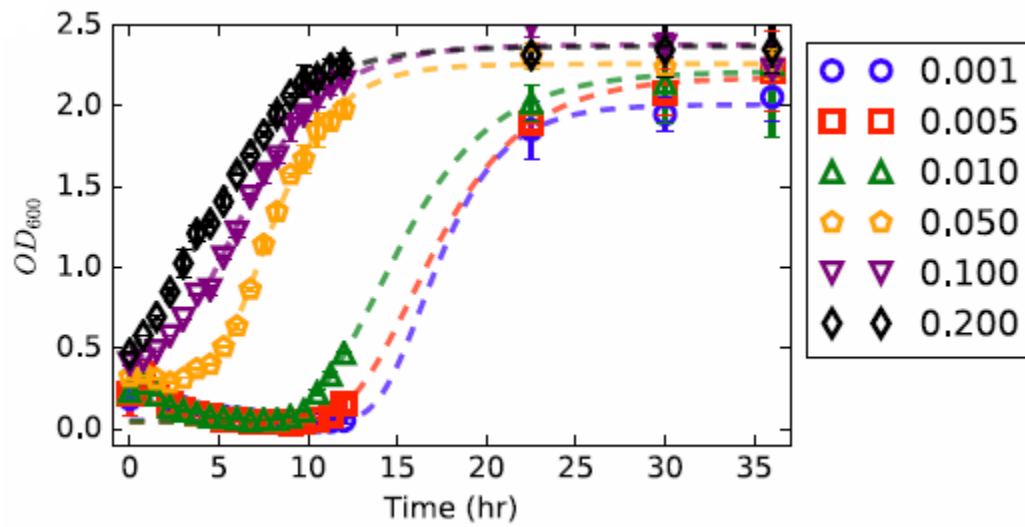


Fig. 4.10: Suppression of bacteria (with different initial concentrations) by AgNPs up to 36 hours

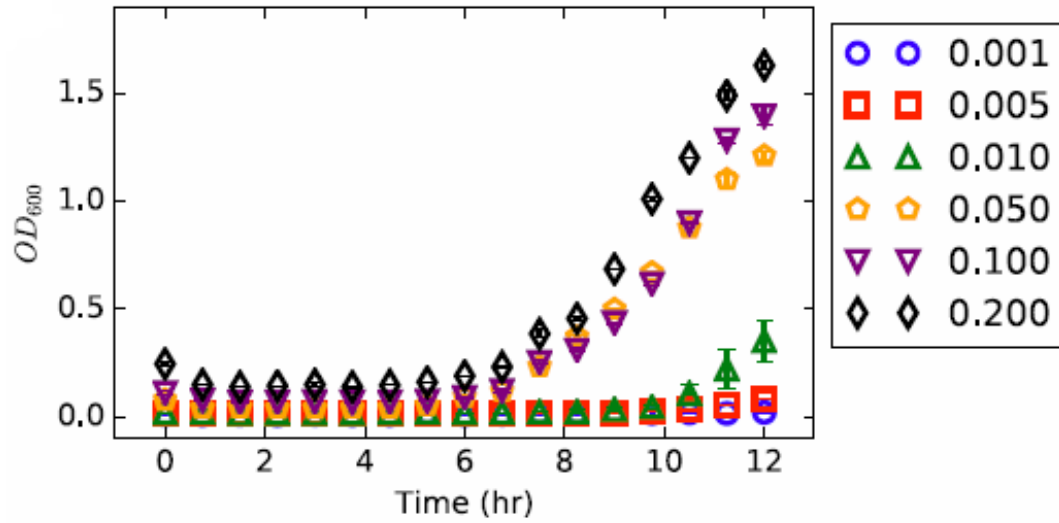


Fig. 4.11: Suppression of bacteria (with different initial concentrations) by Ag^+ ions up to 12 hours

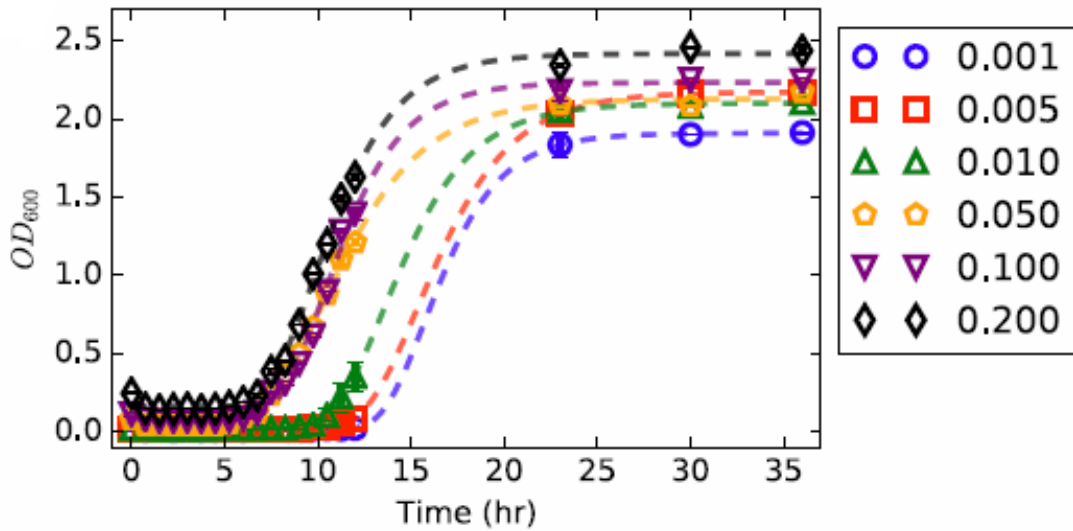


Fig. 4.12: Suppression of bacteria (with different initial concentrations) by Ag^+ ions up to 36 hours

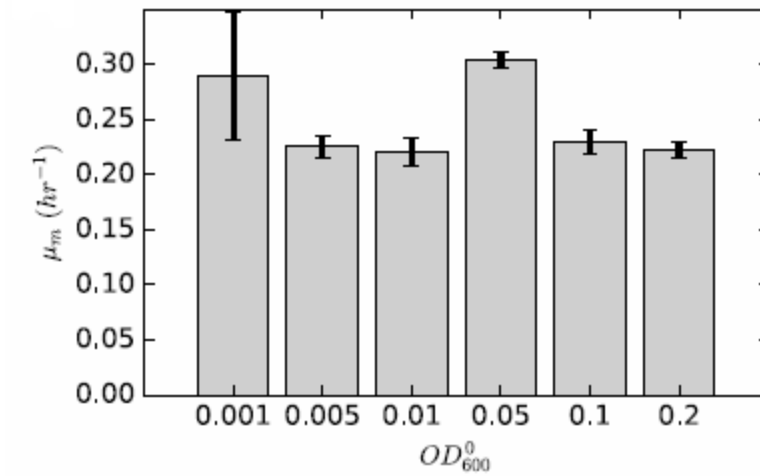


Fig. 4.13: Relation between maximum specific growth rate (μ_m) and initial concentration of bacteria when AgNPs were added

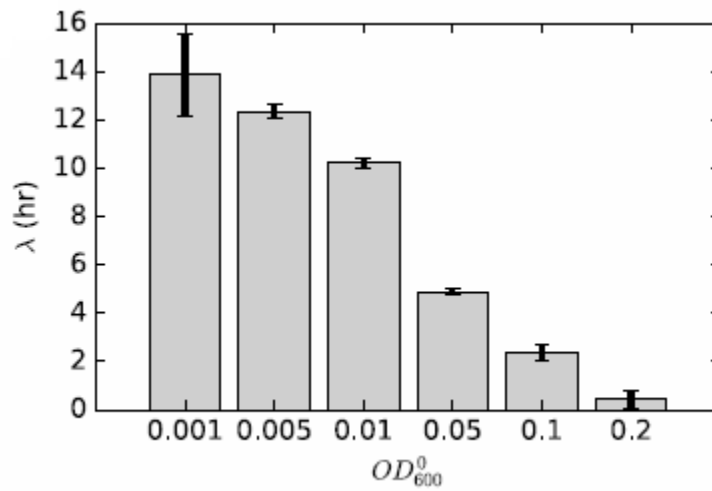


Fig. 4.14: Relation between lag time (λ) and initial concentration of bacteria when AgNPs were added

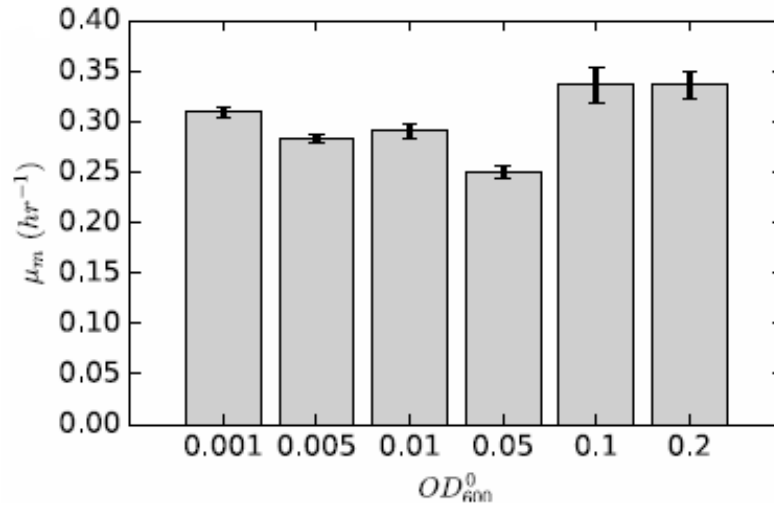


Fig. 4.15: Relation between maximum specific growth rate (μ_m) and initial concentration of bacteria when $AgNO_3$ were added

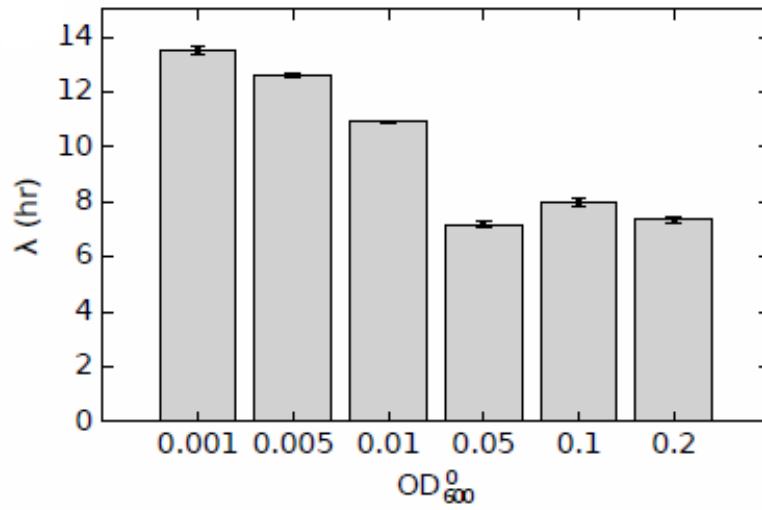


Fig. 4.16: Relation between lag time (λ) and initial concentration of bacteria when $AgNO_3$ were added

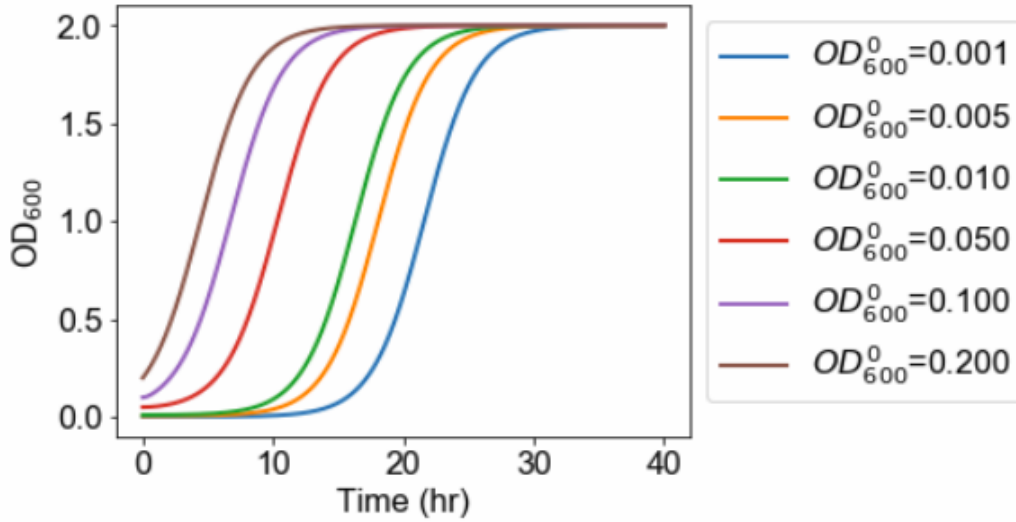


Fig. 4.17: Simulated growth curves using SAD model for different initial OD_{600}

Similarly, the dependence of wake-up rate β on the initial concentration of *E. coli* bacteria cells (estimated as OD_{600} value) can be calculated. For this, kinetic growth assays were performed with fixed initial concentration of AgNPs (20 $\mu\text{g/mL}$) but different initial concentrations of *E. coli* bacteria. It has been observed that the growth curves shifted to the right with the drop of initial concentration of bacteria (Fig 4.9-Fig. 4.12). By fitting the growth curves, we can see that maximum specific growth rates μ_m remains similar (Fig. 4.9-Fig. 4.16). However, the lag time rises with the drop of initial bacterial concentration OD_{600} (Fig. 4.9-Fig. 4.16). The SAD model can reproduce these empirical observations (Fig. 4.17). From this set of growth curves at different initial OD_{600} values, the wake-up rates can be determined. The logarithm of the wake-up rate was also found linear following the equation:

$$\ln\beta = \kappa_d \cdot OD_{600}^0 + \theta_d$$

By curve fitting (Fig. 4.8), the following values were found:

$$\kappa_d = 38 \pm 9 \text{ and}$$

$$\theta_d = -5.2 \pm 0.9$$

The positive slope of curve in Fig. 4.8 indicates that lower initial concentrations of bacteria would result in longer lag phases which is consistent with experimental observation (Fig. 4.13- Fig. 4.16). From the kinetic growth curves, the wake-up rates were found to be exponentially related to the concentrations:

$$\beta = e^{\kappa_S \cdot [AgNP] + \theta_S} \text{ and } \beta = e^{\kappa_D \cdot OD_{600}^0 + \theta_d} \quad (3)$$

Or,

$$\beta = \beta_0 \cdot e^{\kappa_S \cdot [AgNP] + \kappa_D \cdot OD_{600}^0} \quad (4)$$

Where, β_0 is a constant factor consisting of both e^{θ_S} and e^{θ_d} .

We can see that wake-up rate depends on both initial concentration of bacteria and concentration of AgNPs. However, these two dependencies are derived from two independent sets of growth curves (one by varying concentration of AgNP and the other by varying initial concentration of bacteria) although resulting the same characteristic equation (4). Therefore, these two dependencies can be utilized to verify the SAD model. By comparing equation (3) and (4), we see:

$$\left. \begin{aligned} \beta &= e^{\kappa_D \cdot OD_{600}^0 + \theta_d} = \beta_0 \cdot e^{\kappa_S \cdot 20 + \kappa_D \cdot OD_{600}^0} \\ \beta &= e^{\kappa_S \cdot [AgNP] + \theta_s} = \beta_0 \cdot e^{\kappa_S \cdot [AgNP] + \kappa_D \cdot 0.05} \end{aligned} \right\} \quad (5)$$

Which gives-

$$e^{\theta_d} = \beta_0 \cdot e^{\kappa_S \cdot 20} \text{ and } e^{\theta_s} = \beta_0 \cdot e^{\kappa_D \cdot 0.05} \quad (6)$$

As both θ_s and θ_d were derived using $OD_{600}^0 = 0.05$ and $[AgNP] = 20 \mu\text{g/mL}$, if the SAD model is correct, we expect:

$$\theta_s - \theta_d = \kappa_D \cdot 0.05 - \kappa_S \cdot 20 \quad (7)$$

Putting the values obtained for $\theta_s, \theta_d, \kappa_D$ and κ_S , we get

$$\text{LHS} = \theta_s - \theta_d = 9.4 \pm 1.2$$

$$\text{RHS} = \kappa_D \cdot 0.05 - \kappa_S \cdot 20 = 9.7 \pm 0.8$$

It proves that Eqn. 7 is true thereby justifying the model. A sigmoid relation between the killing percentage of bacteria and concentration of AgNPs can be plotted as Fig. 4.18 using the SAD model and the empirical relation between wake-up rate and concentration of AgNPs, $[AgNP]$. Previous experimental works also showed tolerance in cells as the concentration of AgNPs changes [41].

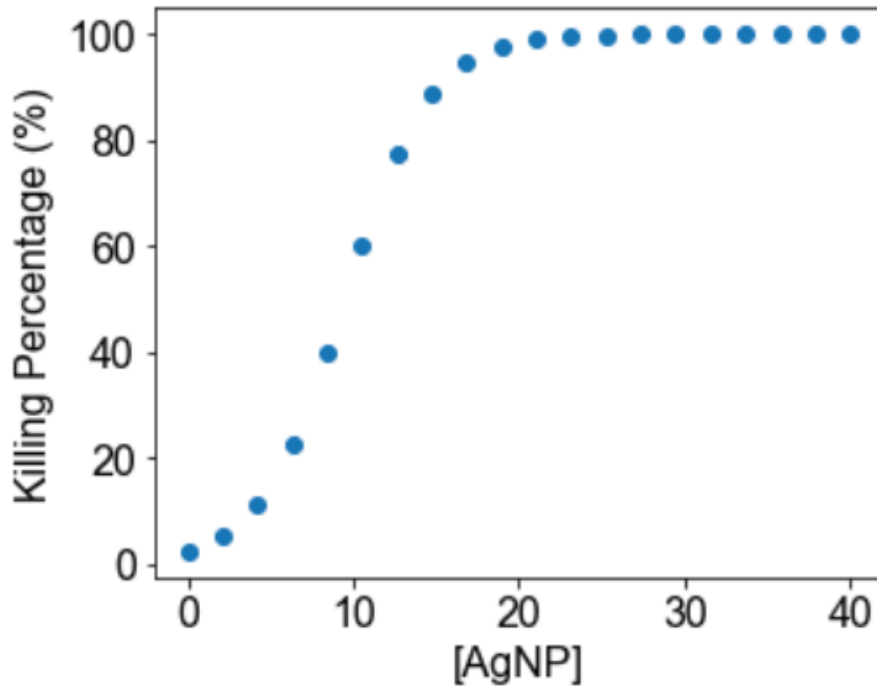


Fig. 4.18: Predicted percentage of killed *E. coli* bacteria as a function of AgNP concentration using the SAD model

CHAPTER FIVE

Discussion and Conclusion

The antimicrobial activity of AgNPs and Ag⁺ were analyzed using kinetic growth curve and CFU assay for *E. coli* bacteria and a quantitative model was formed based on the experimental observations. Kinetic growth assay shows that AgNPs and Ag⁺ ions do not change the maximum specific growth rate but extends the lag time thereby delaying the growth of bacteria. Lag times in kinetic growth assays increase with the increase in concentration of AgNPs and decrease in initial concentration of *E. coli* bacteria. Ag kills some *E. coli* bacteria as we can see from the time-kill curves obtained from the CFU assay. However, the killing rate is apparently independent of AgNP concentration. From the time-kill curves, it was also observed that Ag⁺ ions were more efficient in killing bacteria cells compared to AgNPs.


A quantitative model has been proposed to characterize these antimicrobial characteristics of AgNPs and Ag⁺ ions. This model has been termed as Suppressed-Active-Dead (SAD) model and has some significant features. It can replicate the experimental phenomena (kinetic growth assays and time-kill curves) quite well and hence can potentially be used to predict the antimicrobial activity of AgNPs. The key parameters of the model (killing rate α and wake-up rate β) can be extracted from the experimental data. The dependency of wake-up rate β on the concentration of both AgNPs and *E. coli* bacteria can also be determined experimentally. Finally, the model can be a potentially alternative method to characterize the antimicrobial property of AgNPs and Ag⁺ ions, rather than the conventional Minimum Inhibitory Concentration (MIC) and Minimum Bactericidal Concentration (MBC) methods.

On the other hand, this model has some limitations. Our model is based on experimental phenomena and can predict the outcome of AgNPs and *E. coli* interaction. It can neither explain how bacteria are pushed to and contained in the suppressed state nor describe the mechanism of the suppressed state at the molecular level. Moreover, how bacteria cope up with the suppressed state and wake up to regrow are not explicable by the model. Further investigations at molecular level are required to explain these mechanisms. An immediate future work might be the use of different shapes of nanoparticles to explore how the shapes and sizes affect the maximum specific growth and lag time in kinetic growth of bacteria. While conducting the presented research, the opacity of AgNP solution was a problem in kinetic growth curve assays. Use of a more advanced instrument might be helpful to determine the concentration of the solution in kinetic growth assays without being affected by nanoparticle concentration. Besides, the presented work included only the effect on *Escherichia coli*. The effect on other microorganisms must be explored to observe whether this is a unique feature of *E. coli* suppression by AgNPs or AgNPs are capable of suppressing other types of bacteria also. The effect on lag time and maximum growth rate for other bacteria needs to be analyzed to see its difference with antibiotics in case of different types of bacteria.

Although previous works included the change in cell physiology with the introduction of nanoparticles, the use of super resolution spectroscopy can be a good tool to investigate the mechanism of bacteria suppression by AgNPs and how bacteria climb up through the suppressed state and start to regrow. Moreover, it will help to understand the resistive nature in bacteria and how bacteria have been able to cope up with antibiotics for ages so that preventive measure can be taken.

References

- [1] R. D. Forrest, “Early history of wound treatment.,” *J. R. Soc. Med.*, vol. 75, no. 3, pp. 198–205, 1982.
- [2] W. Foster and A. Raoult, “Early descriptions of antibiosis.,” *J. R. Coll. Gen. Pract.*, vol. 24, no. 149, pp. 889–94, 1974.
- [3] J. Straand, C. Gradmann, M. Lindbæk, and G. S. Simonsen, “Antibiotic development and resistance,” in *International Encyclopedia of Public Health*, 2008, pp. 200–211.
- [4] S. Y. Tan and Y. Tatsumura, “Alexander Fleming (1881–1955): Discoverer of penicillin,” *Singapore Med. J.*, vol. 56, no. 7, pp. 366–367, 2015.
- [5] S. H. W. Florey, “THE USE OF MICRO-ORGANISMS FOR THERAPEUTIC PURPOSES,” *Br. Med. J.*, pp. 635–642, 1945.
- [6] H. L. Van Epps, “René Dubos: unearthing antibiotics,” *J. Exp. Med.*, vol. 203, no. 2, pp. 259–259, 2006.
- [7] A. Griffiths, S. Wessler, R. Lewontin, W. Gelbart, D. Suzuki, and J. Miller, “An introduction to genetic analysis,” *Vasa*, p. 706, 2005.
- [8] O. Tenaillon, D. Skurnik, B. Picard, and E. Denamur, “The population genetics of commensal *Escherichia coli*,” *Nat. Rev. Microbiol.*, vol. 8, no. 3, pp. 207–217, 2010.
- [9] “*Escherichia coli* - Redorbit.” [Online]. Available: http://www.redorbit.com/reference/escherichia_coli/. [Accessed: 03-Jul-2017].
- [10] U. Fotadar, P. Zaveloff, and L. Terracio, “Growth of *Escherichia coli* at elevated temperatures,” *J. Basic Microbiol.*, vol. 45, no. 5, pp. 403–404, 2005.
- [11] W. J. Ingledew and R. K. Poole, “The respiratory chains of *Escherichia coli*,” *Microbiol. Rev.*, vol. 48, no. 3, pp. 222–271, 1984.
- [12] B. R. Funke and C. L. Case, *Microbiology An Introduction*, 10th ed. San Francisco: Pearson Education, [nc., 2010.
- [13] R. Bentley and R. Meganathan, “Biosynthesis of vitamin K (menaquinone) in bacteria.,” *Microbiol. Rev.*, vol. 46, no. 3, pp. 241–280, 1982.
- [14] R. L. Vogt and L. Dippold, “*Escherichia coli* O157:H7 outbreak associated with consumption of ground beef, June-July 2002.,” *Public Health Rep.*, vol. 120, no. 2, pp. 174–178, 2005.
- [15] C. J. Lim, Ji Youn; Yoon, Jang W.; Hovde, “A brief overview of *Escherichia coli* O157:H7 and Its Plasmid O157,” *J. Microbiol. Biotechnol.*, vol. 20, no. 1, pp. 5–14, 2010.

- [16] “WHO | E. coli,” *WHO*, 2016.
- [17] “Shiga Toxin-Producing E. coli & Food Safety | Features | CDC,” 2017. [Online]. Available: <https://www.cdc.gov/features/ecoliinfection/>. [Accessed: 03-Jul-2017].
- [18] “Pediatric Emergency Medicine Practice Acute Gastroenteritis  An Update,” 2010. [Online]. Available: http://www.ebmedicine.net/topics.php?paction=showTopic&topic_id=229. [Accessed: 06-Jul-2017].
- [19] “Get Smart About Antibiotics | Urinary Tract Infection | CDC,” 2015. [Online]. Available: <https://www.cdc.gov/getsmart/community/for-patients/common-illnesses/uti.html#>. [Accessed: 03-Jul-2017].
- [20] D. R. Lane and S. S. Takhar, “Diagnosis and Management of Urinary Tract Infection and Pyelonephritis,” *Emergency Medicine Clinics of North America*, vol. 29, no. 3. pp. 539–552, 2011.
- [21] A. A. Al-Harhi, K. A. Dagriri, A. A. Asindi, and C. S. Bello, “Neonatal meningitis.,” *Saudi Med. J.*, vol. 21, no. 6, pp. 550–553, 2000.
- [22] M. C. Lin, H. Chi, N. C. Chiu, F. Y. Huang, and C. S. Ho, “Factors for poor prognosis of neonatal bacterial meningitis in a medical center in Northern Taiwan,” *J. Microbiol. Immunol. Infect.*, vol. 45, no. 6, pp. 442–447, 2012.
- [23] T. Phillips, “Reasons E. coli Is Used for Gene Cloning,” 2017. [Online]. Available: <https://www.thebalance.com/top-reasons-e-coli-is-used-for-gene-cloning-375742>. [Accessed: 06-Jul-2017].
- [24] M. T. Madigan, J. M. Martinko, and J. Parker, *Brock Biology of Microorganisms, 10th Edition*, vol. 2. 2003.
- [25] S. Chernousova and M. Epple, “Silver as antibacterial agent: Ion, nanoparticle, and metal,” *Angewandte Chemie - International Edition*, vol. 52, no. 6. pp. 1636–1653, 2013.
- [26] A. J.W., “History of the medical use of silver,” *Surgical Infections*, vol. 10, no. 3. pp. 289–292, 2009.
- [27] W. K. Jung, H. C. Koo, K. W. Kim, S. Shin, S. H. Kim, and Y. H. Park, “Antibacterial Activity and Mechanism of Action of the Silver Ion in Staphylococcus aureus and Escherichia coli,” *Appl. Environ. Microbiol.*, vol. 74, no. 7, pp. 2171–2178, 2008.
- [28] H. C. Neu, “The Crisis in Antibiotic Resistance,” *Science (80-.)*, vol. 257, no. 5073, pp. 1064–1073, 1992.
- [29] X. Li *et al.*, “Functional gold nanoparticles as potent antimicrobial agents against multi-drug-resistant bacteria,” *ACS Nano*, vol. 8, no. 10, pp. 10682–10686, 2014.

- [30] B. Le Ouay and F. Stellacci, "Antibacterial activity of silver nanoparticles: A surface science insight," *Nano Today*, vol. 10, no. 3. pp. 339–354, 2015.
- [31] Y. Zhou, Y. Kong, S. Kundu, J. D. Cirillo, and H. Liang, "Antibacterial activities of gold and silver nanoparticles against *Escherichia coli* and *Bacillus Calmette-Guérin*," *J. Nanobiotechnology*, vol. 10, no. 1, p. 19, 2012.
- [32] R. Geethalakshmi and D. V. L. Sarada, "Characterization and antimicrobial activity of gold and silver nanoparticles synthesized using saponin isolated from *Trianthema decandra* L.," *Ind. Crops Prod.*, vol. 51, pp. 107–115, 2013.
- [33] J. Liu and R. H. Hurt, "Ion release kinetics and particle persistence in aqueous nano-silver colloids," *Environ. Sci. Technol.*, vol. 44, no. 6, pp. 2169–2175, 2010.
- [34] J. Liu, D. A. Sonshine, S. Shervani, and R. H. Hurt, "Controlled release of biologically active silver from nanosilver surfaces," *ACS Nano*, vol. 4, no. 11, pp. 6903–6913, 2010.
- [35] B. Nowack, H. F. Krug, and M. Height, "120 years of nanosilver history: Implications for policy makers," *Environ. Sci. Technol.*, vol. 45, no. 4, pp. 1177–1183, 2011.
- [36] S. Prabhu and E. K. Poulouse, "Silver nanoparticles: mechanism of antimicrobial action, synthesis, medical applications, and toxicity effects," *Int. Nano Lett.*, vol. 2, no. 1, p. 32, 2012.
- [37] B. J. Wiley, Y. Xiong, Z. Y. Li, Y. Yin, and Y. Xia, "Right bipyramids of silver: A new shape derived from single twinned seeds," *Nano Lett.*, vol. 6, no. 4, pp. 765–768, 2006.
- [38] E. Hao, K. L. Kelly, J. T. Hupp, and G. C. Schatz, "Synthesis of silver nanodisks using polystyrene mesospheres as templates," *J. Am. Chem. Soc.*, vol. 124, no. 51, pp. 15182–15183, 2002.
- [39] C. Ni, P. A. Hassan, and E. W. Kaler, "Structural characteristics and growth of pentagonal silver nanorods prepared by a surfactant method," *Langmuir*, vol. 21, no. 8, pp. 3334–3337, 2005.
- [40] D. D. Evanoff and G. Chumanov, "Synthesis and optical properties of silver nanoparticles and arrays," *ChemPhysChem*, vol. 6, no. 7. pp. 1221–1231, 2005.
- [41] Z. Xiu, Q. Zhang, H. L. Puppala, V. L. Colvin, and P. J. J. Alvarez, "Negligible particle-specific antibacterial activity of silver nanoparticles," *Nano Lett.*, vol. 12, no. 8, pp. 4271–5, 2012.
- [42] P. V. AshaRani, G. L. K. Mun, M. P. Hande, and S. Valiyaveetil, "Cytotoxicity and genotoxicity of silver nanoparticles in human cells," *ACS Nano*, vol. 3, no. 2, pp. 279–290, 2009.
- [43] S. Kittler, C. Greulich, J. Diendorf, M. Köller, and M. Epple, "Toxicity of silver

- nanoparticles increases during storage because of slow dissolution under release of silver ions,” *Chem. Mater.*, vol. 22, no. 16, pp. 4548–4554, 2010.
- [44] N. R. Panyala, E. M. Peña-Méndez, and J. Havel, “Silver or silver nanoparticles: a hazardous threat to the environment and human health?,” *J. Appl. Biomed.*, vol. 6, no. 3, pp. 117–129, 2008.
- [45] I. Sondi and B. Salopek-Sondi, “Silver nanoparticles as antimicrobial agent: A case study on *E. coli* as a model for Gram-negative bacteria,” *J. Colloid Interface Sci.*, vol. 275, no. 1, pp. 177–182, 2004.
- [46] S. Agnihotri, S. Mukherji, and S. Mukherji, “Size-controlled silver nanoparticles synthesized over the range 5–100 nm using the same protocol and their antibacterial efficacy,” *RSC Adv.*, vol. 4, no. 8, pp. 3974–3983, 2014.
- [47] S. Pal, Y. K. Tak, and J. M. Song, “Does the antibacterial activity of silver nanoparticles depend on the shape of the nanoparticle? A study of the gram-negative bacterium *Escherichia coli*,” *J. Biol. Chem.*, vol. 290, no. 42, pp. 1712–1720, 2015.
- [48] A. F. Anaerobe, R. Krishnan, V. Arumugam, and S. K. Vasaviah, “The MIC and MBC of Silver Nanoparticles against *Enterococcus faecalis* - A Facultative Anaerobe,” *J. Nanomed. Nanotechnol.*, vol. 6, no. 3, 2015.
- [49] J. S. Kim *et al.*, “Antimicrobial effects of silver nanoparticles,” *Nanomedicine Nanotechnology, Biol. Med.*, vol. 3, no. 1, pp. 95–101, 2007.
- [50] H. Lodish, A. Berk, S. L. Zipursky, P. Matsudaira, D. Baltimore, and J. Darnell, *Molecular Cell Biology. 4th edition.* 2000.
- [51] Z. Cai, N. Chattopadhyay, W. J. Liu, C. Chan, J.-P. Pignol, and R. M. Reilly, “Optimized digital counting colonies of clonogenic assays using ImageJ software and customized macros: Comparison with manual counting,” *Int. J. Radiat. Biol.*, vol. 87, no. 11, pp. 1135–1146, 2011.
- [52] a Simon-Deckers, “Size-, composition-and shape-dependent toxicological impact of metal oxide nanoparticles and carbon nanotubes toward bacteria,” ... *Sci. Technol.*, pp. 1–6, 2009.
- [53] Q. L. Feng, J. Wu, G. Q. Chen, F. Z. Cui, T. N. Kim, and J. O. Kim, “A mechanistic study of the antibacterial effect of silver ions on *Escherichia coli* and *Staphylococcus aureus*,” *Journal of Biomedical Materials Research*, vol. 52, no. 4, pp. 662–668, 2000.
- [54] B. Alberts, A. Johnson, J. Lewis, M. Raff, K. Roberts, and P. Walter, *Molecular Biology of the Cell.* 2002.
- [55] J. Brennan, “The Difference Between Genomic DNA & Plasmid DNA | Sciencing,” 2017. [Online]. Available: <http://sciencing.com/difference-between-genomic-dna-plasmid-dna-2314.html>. [Accessed: 11-Jul-2017].

- [56] “Bacterial DNA – the role of plasmids — Science Learning Hub,” 2014. [Online]. Available: <https://www.sciencelearn.org.nz/resources/1900-bacterial-dna-the-role-of-plasmids>. [Accessed: 11-Jul-2017].
- [57] Y. Zhao, Y. Tian, Y. Cui, W. Liu, W. Ma, and X. Jiang, “Small-Molecule Capped Gold Nanoparticles as Potent Antibacterial Agents that Target Gram-negative Bacteria,” *J. Am. Chem. Soc.*, vol. 132, no. 24, pp. 12349–12356, 2010.
- [58] Y. Cui, Y. Zhao, Y. Tian, W. Zhang, X. Lü, and X. Jiang, “The molecular mechanism of action of bactericidal gold nanoparticles on Escherichia coli,” *Biomaterials*, vol. 33, no. 7, pp. 2327–2333, 2012.
- [59] S. Lacour, “Emerging questions for emerging technologies: Is there a law for the nano?,” *Nanomater. A Danger or a Promise? A Chem. Biol. Perspect.*, pp. 357–378, 2013.
- [60] S. Lacour, *Nanomaterials: A Danger or a Promise?* 2013.
- [61] B. J. Berne and R. Pecora, *Dynamic Light Scattering: With Applications to Chemistry, Biology, and Physics*. 2003.
- [62] M. Instruments, “Inform White Paper Dynamic Light Scattering,” *Malvern Guid.*, pp. 1–6, 2011.
- [63] W. Slavin, “Atomic-Absorption Spectroscopy? a Critical Review,” *Appl. Spectrosc.*, vol. 20, no. 5, pp. 281–288, 1966.
- [64] “Introduction: X-Ray Diffraction.”
- [65] “electrokinetic potential, ?,” in *IUPAC Compendium of Chemical Terminology*, Research Triangle Park, NC: IUPAC, 2008.
- [66] K. L. Huynh, Khanh An; Chen, “Aggregation Kinetics of Citrate and Polyvinylpyrrolidone Coated Silver Nanoparticles in Monovalent and Divalent Electrolyte Solutions,” *Environ. Sci. Technol.*, vol. 45, no. 13, pp. 5564–5571, 2012.
- [67] (World Health Organization) WHO, “WHO.WHOModel Lists of Essential Medicines. In: Essential medicines and health products,” *Intermet*, vol. 19, no. April, pp. 1–43, 2015.
- [68] R. Y. Tsien, “The green fluorescent protein,” *Annu. Rev. Biochem.*, vol. 67, pp. 509–544, 1998.
- [69] G. Sezonov, D. Joseleau-Petit, and R. D’Ari, “Escherichia coli physiology in Luria-Bertani broth,” *J. Bacteriol.*, vol. 189, no. 23, pp. 8746–8749, 2007.
- [70] J. K. Maiti, Swarnali ; Krishnan, Deepak; Barman, Gadadhar; Ghosh, Sudip Kumar; Laha, “Antimicrobial activities of silver nanoparticles synthesized from Lycopersicon esculentum extract,” *J. Anal. Sci. Technol.*, vol. 25, no. 18, pp. 4383–4391, 2004.

- [71] M. H. Zwietering, I. Jongenburger, F. M. Rombouts, and K. van 't Riet, "Modeling of the bacterial growth curve.," *Appl. Environ. Microbiol.*, vol. 56, no. 6, pp. 1875–81, 1990.
- [72] B. Gompertz, "On the Nature of the Function Expressive of the Law of Human Mortality, and on a New Mode of Determining the Value of Life Contingencies," vol. 115, pp. 513–583, 1825.
- [73] F. J. Richards, "A Flexible Growth Function for Empirical Use," *J. Exp. Botany*, vol. 10, pp. 290–300, 1959.
- [74] J. Schnute, "A versatile growth model with statistically stable parameters," *Can. J. Fish. Aquat. Sci.*, vol. 38, no. 9, pp. 1128–1140, 1981.
- [75] B. Li, Y. Qiu, H. Shi, and H. Yin, "The importance of lag time extension in determining bacterial resistance to antibiotics," *Analyst*, vol. 141, no. 10, pp. 3059–3067, 2016.
- [76] H. Bao *et al.*, "New toxicity mechanism of silver nanoparticles: Promoting apoptosis and inhibiting proliferation," *PLoS One*, vol. 10, no. 3, 2015.
- [77] A. Juska, G. Gedminiene, and R. Ivanec, "Growth of microbial populations: Mathematical modeling, laboratory exercises, and model-based data analysis," *Biochem. Mol. Biol. Educ.*, vol. 34, no. 6, pp. 417–422, 2006.
- [78] C. Begot, I. Desnier, J. D. Daudin, J. C. Labadie, and A. Lebert, "Recommendations for calculating growth parameters by optical density measurements," *J. Microbiol. Methods*, vol. 25, no. 3, pp. 225–232, 1996.
- [79] G. A. Pankey and L. D. Sabath, "Clinical Relevance of Bacteriostatic versus Bactericidal Mechanisms of Action in the Treatment of Gram-Positive Bacterial Infections," *Clin. Infect. Dis.*, vol. 38, no. 6, pp. 864–870, 2004.
- [80] Y. Zhang, "Persisters, persistent infections and the Yin–Yang model," *Emerg. Microbes Infect.*, vol. 3, no. 1, p. e3, 2014.

Appendix



April 15, 2016

MEMORANDUM

TO: Dr. Yong Wang

FROM: Ines Pinto, Biosafety Committee Chair

RE: New Protocol

PROTOCOL #: 16037

PROTOCOL TITLE: single-cell Elucidation of mechanism behind plasmid maintenance in bacteria at level

APPROVED PROJECT PERIOD: Start Date April 14, 2016 Expiration Date April 13, 2019

The Institutional Biosafety Committee (IBC) has approved Protocol 16037, "Elucidation of mechanism behind plasmid maintenance in bacteria at single-cell level". You may begin your study.

If modifications are made to the protocol during the study, please submit a written request to the IBC for review and approval before initiating any changes.

The IBC appreciates your assistance and cooperation in complying with University and Federal guidelines for research involving hazardous biological materials.



UNIVERSITY OF
ARKANSAS

Research & Economic Development
Research Compliance

July 14, 2017

MEMORANDUM

TO: Dr. Yong Wang

FROM: Ines Pinto, Biosafety Committee Chair

RE: New Protocol

PROTOCOL #: 18004

PROTOCOL TITLE: Physically-based, single-cell investigation of bacterial response to environment changes

APPROVED PROJECT PERIOD: Start Date July 13, 2017 Expiration Date July 12, 2020

The Institutional Biosafety Committee (IBC) has approved Protocol 18004, “Physically-based, single-cell investigation of bacterial response to environment changes”. You may begin your study.

If modifications are made to the protocol during the study, please submit a written request to the IBC for review and approval before initiating any changes.

The IBC appreciates your assistance and cooperation in complying with University and Federal guidelines for research involving hazardous biological materials.